

Review

# Advancements and Future Prospects of Buckling Restrained Braces for Corrosive-Environments: A Comprehensive Literature Review

Hubdar Hussain <sup>1</sup>  and Dong-Keon Kim <sup>1,2,\*</sup>

<sup>1</sup> Department of ICT Integrated Ocean Smart Cities Engineering, Dong-A University, Busan 49304, Republic of Korea

<sup>2</sup> National Core Research Center for Disaster-Free and Safe Ocean Cities Construction, Dong-A University, Busan 49304, Republic of Korea

\* Correspondence: dkkzone@dau.ac.kr

**Abstract:** The seismic design of structures is crucial for preventing structural collapse and safeguarding human lives. Buckling-restrained braces (BRBs) have emerged as effective seismic protection devices due to their high stiffness, strength, and exceptional energy absorption capabilities. Typically, a conventional BRB consists of a steel core surrounded by concrete-filled steel tubes, with a separation mechanism ensuring axial-only deformation of the core. However, researchers have been increasingly focusing on developing innovative BRB designs with enhanced performance, incorporating different materials and configurations. This paper presents a comprehensive analysis of the development of novel BRBs introduced in the past 15 years. A systematic review approach is adopted, and the selected articles are categorized based on the shapes, materials, and compositions of the BRB components. Although carbon steel has been widely used in numerous studies, its susceptibility to corrosion and its potential impact on the hysteretic behavior of BRBs remain unexplored. Consequently, future research prospects are identified, highlighting the significance of employing anti-corrosive materials in fabricating BRBs to ensure their stable seismic performance under harsh environmental conditions. Investigating novel materials and configurations can lead to the creation of more robust and corrosion-resistant BRBs, thus enhancing the safety and longevity of structures in earthquake-prone areas.

**Keywords:** seismic design; seismic protection devices; buckling-restrained braces; anti-corrosive materials; corrosion-resistant BRBs; earthquake-prone areas



**Citation:** Hussain, H.; Kim, D.-K. Advancements and Future Prospects of Buckling Restrained Braces for Corrosive-Environments: A Comprehensive Literature Review. *Buildings* **2023**, *13*, 2156. <https://doi.org/10.3390/buildings13092156>

Academic Editors: Wusheng Zhao and Magdalini D. Titirila

Received: 8 June 2023

Revised: 29 July 2023

Accepted: 23 August 2023

Published: 25 August 2023



**Copyright:** © 2023 by the authors. Licensee MDPI, Basel, Switzerland. This article is an open access article distributed under the terms and conditions of the Creative Commons Attribution (CC BY) license (<https://creativecommons.org/licenses/by/4.0/>).

## 1. Introduction

Natural disasters such as frequent earthquakes pose a serious threat to human life and drastically influence the economy of a country [1–3]. Effective aseismic structural systems always have been an important challenge for engineers. During the past few decades, various types of earthquake-resisting techniques have been developed for the protection of structures by limiting movements during seismic events [4–15]. Additional energy dissipation devices such as braces, dampers, shear links, and shear walls are employed to protect the structures from collapse by dissipating earthquake energy [16–26]. The application of steel braces in high-rise buildings is an effective way to resist seismic forces. Ordinary steel braces provide good performance in the event of a small earthquake, but they undergo buckling deformations and demonstrate unsymmetrical hysteretic response in compression and tension when subjected to large cyclic loads [27,28]. This effect deteriorates the strength of ordinary steel braces substantially and reduces their ability to dissipate seismic energy as shown in Figure 1a. BRBs were developed to restrain the buckling deformation of conventional steel braces and withstand applied loads efficiently [29–31]. These braces

exhibit the same strength under compressive and tensile forces and absorb more energy as compared to ordinary steel braces Figure 1b.

Research on BRBs started in Japan in the 1970s. Yoshino et al. [32] conducted pioneer experiments on flat steel plates surrounded by reinforced concrete panels with a concept of “steel reinforced concrete shear walls with braces”.

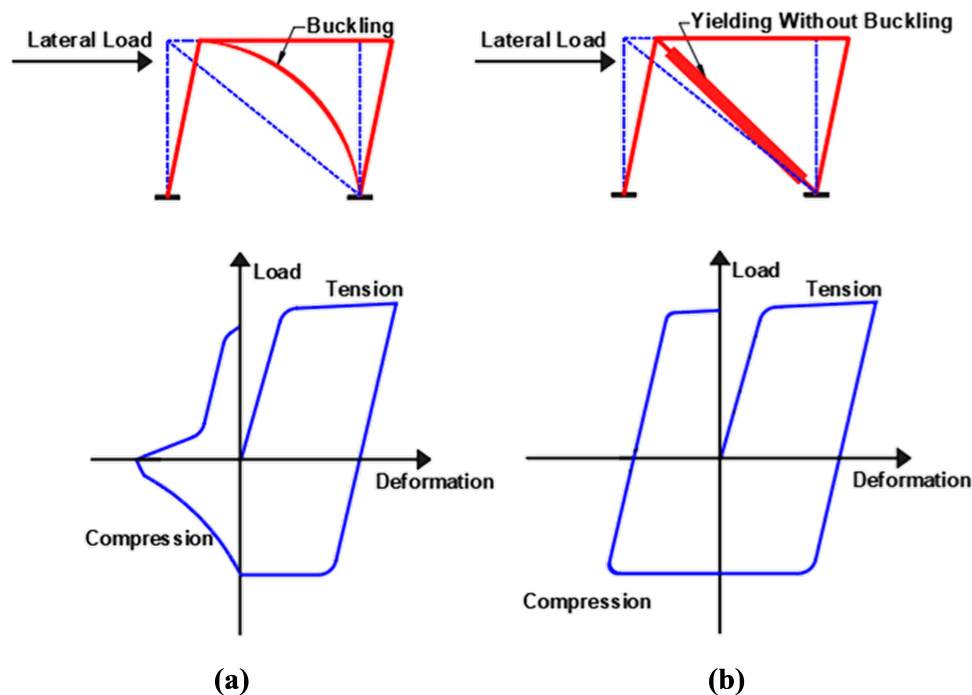


Figure 1. Response of ordinary steel brace and BRB under lateral loading [33].

Subsequently, many researchers [34–36] keep working on the same idea, and in 1988, Fujimoto et al. [37], and a team from Nippon Steel Company developed the first practical form of the currently adopted BRB. Poor performance of moment-resisting frames (MRF) and steel-braced frames during the Northridge and Kobe earthquakes also attracted the research community’s attention to investigate the seismic behavior of BRB frames and explore their potential benefits as earthquake-resisting systems [38–40]. As a result of their effective performance and stable hysteretic response under cyclic loading, BRBs gained popularity and magnetized the interest of other countries’ researchers. It is now broadly utilized worldwide in many countries such as the U.S., Canada, China, Turkey, Chile, and New Zealand [41–43].

The regular structure of a conventional BRB generally consists of four parts: a core component, unbonding material, infilled material, and an exterior restraining unit as shown in Figure 2. Regardless of the exceptional ductility and energy dissipation of conventional BRBs, these braces have some drawbacks. The braces become heavier due to the presence of concrete/mortar and create problems inspecting the damaged core after earthquakes [44]. Subsequently, different forms of BRBs with restraining parts mainly made of steel, labeled as all-steel BRBs, have been proposed by numerous researchers in the last few years.

Steel BRBs are getting increasing preference from engineers and manufacturers, owing to their enhanced performance and unique specifications, such as lighter weight, shorter manufacturing duration, and easy assembling and disassembling requirements for maintenance and inspection [45,46]. A steel BRB consists of an internal core with a separation unit in the form of a thin layer of unbonding material or pure gap restrained by an external restraining component. The core element of the BRBs withstands the entire axial load and consists of three different segments along its length. The central region, also known as the yielding section, has a reduced cross-section to undergo inelastic deformation for energy dissipation. At both ends of the yielding part, there are two transition segments

with a larger area than the yielding zone to resist the axial demands and remain elastic. Furthermore, the area of the connection parts is increased to connect the BRBs with the structural frame through gusset plates, thereby avoiding stress concentrations [47]. The external restraining component prevents the core from buckling in compression and the separation unit facilitates the smooth axial-only deformation of the central core within the restraining member [48]. The overall efficiency of the Steel-BRB mainly depends on the inelastic deformation capacity of the brace core under repetitive cyclic loading and the stability of the exterior restraining unit [49].

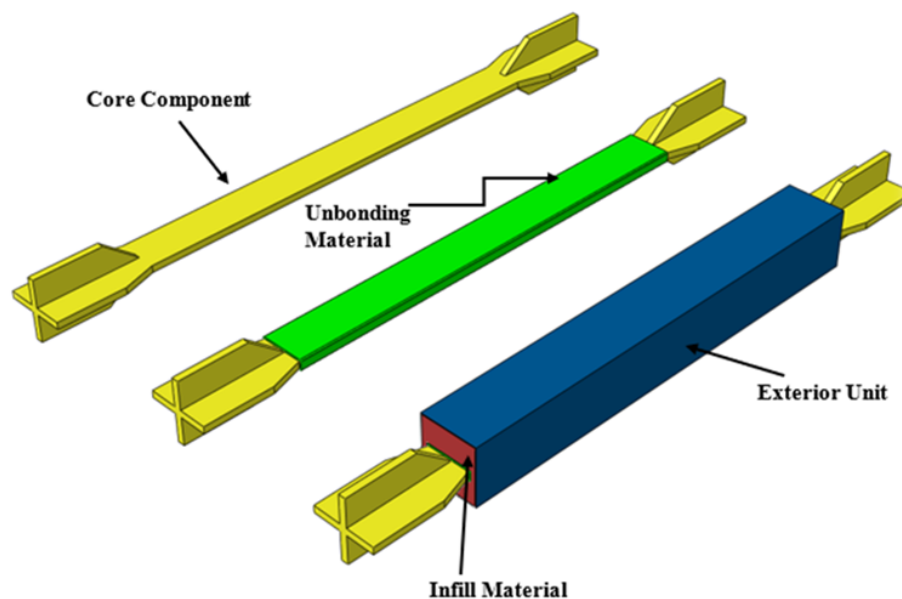


**Figure 2.** Components of conventional BRB [50].

Despite the structural advantages of the steel-BRBs, when BRB frames are employed in coastal areas and humid environments, the outer steel restraining component may become vulnerable because steel corrodes with the passage of time and results in mass loss as well as deterioration of the mechanical properties of the steel [51–56]. To cope with this corrosion issue of the braces, there is a need to develop a better anti-corrosive response of BRBs using alternative materials, such as aluminum-alloys, stainless-steel, shape-memory alloys, and fiber-reinforced polymers (FRP) [57,58].

Efforts are continuing to overcome the inadequacies of BRBs and improve their seismic performance by adopting novel approaches. A state-of-the-art review was presented by Xie on the research and developments of various types of BRBs with different designs in Asia, mainly in Japan [33]. Most recently, Shedge et al. [59] presented a state-of-the-art study on the history and design of BRBs. However, a broad systematic literature review (SLR) on the development of conventional BRBs, all-steel BRBs, and their response under cyclic loadings (with controlled-corroded restraining components) has not been published yet. Thus, this systematic literature review presents a comprehensive analysis of the past 15 years of studies conducted to develop conventional BRBs and all-steel BRBs with an emphasis on the techniques to protect the braces from corrosion. This paper is structured into five sections. Section 2 introduces the methodology for a systematic review to search and identify the relevant research findings. Section 3 analyzes the experimental and numerical studies conducted to develop BRBs and categorizes them based on their main components. Section 4 focuses on the application of anti-corrosive materials in the manufacturing of BRBs. Section 5 presents the conclusions and recommendations for future research on BRBs under corrosive environments.

## 2. Systematic Review Methodology

Systematic reviews have progressively been endorsed by researchers due to their impartiality and understandable nature. Systematic literature reviews (SLR) can assist the scientific community to reproduce the evidence and examine the status of their research field by following a systematized protocol [60,61]. In the literature, several guidelines and approaches have been proposed to perform systematic reviews in a transparent and well-defined manner. This study adopted the systematic literature review methodology recommended by Gregory et al. [62] based on Preferred Reporting Items for Systematic Reviews and Meta-Analyses (PRISMA) guidelines.

### 2.1. Search Strategy

As illustrated in Figure 3, the adopted protocol entails four steps: (1) Identification and Information sources, (2) Screening, (3) Eligibility, and (4) Included. In the first step, six popular publishers and a citation index database were considered to locate the most relevant publications, namely ASCE Library, ScienceDirect, Springer Link, MDPI, Taylor & Francis Online, Willey Online Library, and Web of Science. A wide range of complete scientific works was available in these scientific digital databases and included literature related to BRBs published in high-quality journals. The search queries (“BRB” or “All-steel BRB” or “Buckling Restrained Braces” or “All-steel Buckling Restrained Braces”) AND (“Corrosion”) were formulated and employed to find them in the article/ abstract/ keywords using the advanced features available in online databases.

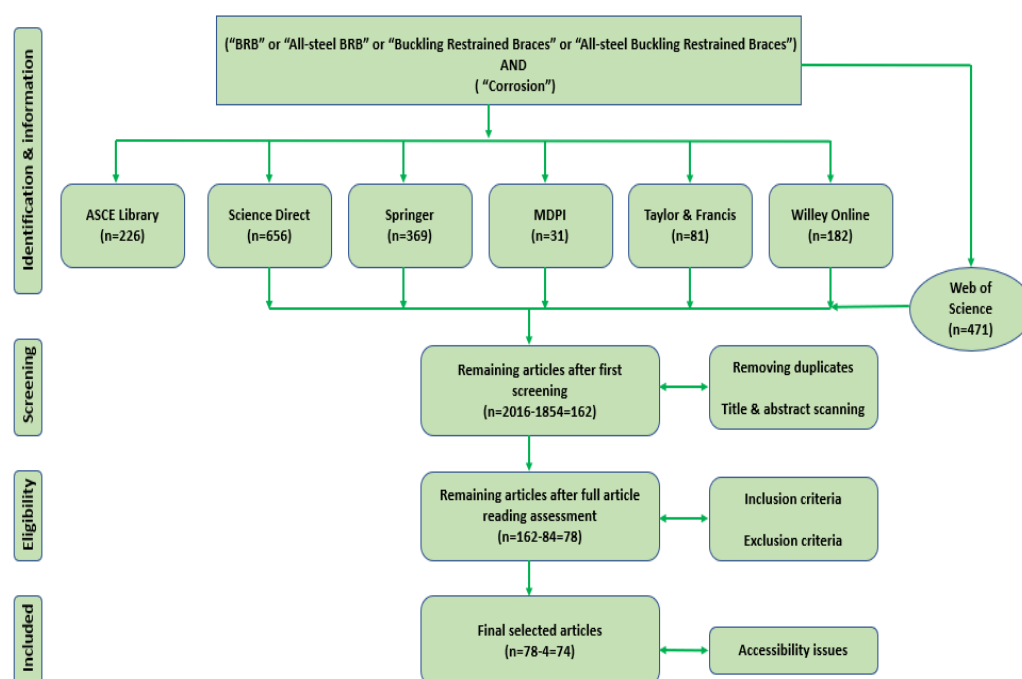


Figure 3. Systematic literature review protocol [62].

The first identification step resulted in 2016 articles. In the next step, duplicate articles (present in more than one database) were removed with the purpose of avoiding counting the same article twice. In addition to this, the title and abstract were examined to figure out the relevant articles based on the research objectives, and 1854 articles were excluded in the screening step. Following the screening stage, the remaining 162 articles were subjected to a second and more detailed filtering to determine whether they met the inclusion and exclusion criteria (Table 1). After thoroughly reviewing, 84 articles were excluded. As a result of the above two processing steps, a total of 1938 articles were eliminated and in the

last step, four more articles were excluded despite fulfilling the acceptance criteria due to inaccessibility issues. Finally, 74 articles were selected for the detailed review.

**Table 1.** Inclusion and exclusion criteria.

| Criteria           | Inclusion   | Exclusion   |
|--------------------|---|---|
| Period             | 2009–2023   | Documents published before 2009   |
| Language           | Language of documents must be English                         | Documents published in other languages                                  |
| Type of document   | Only research articles published in journals of the databases | Other documents (book chapters, conferences, reviews, and proceedings)  |
| Relevance to topic | Articles aimed to develop BRBs with novel aspects             | Articles investigated different parameters of previously developed BRBs |
| Availability       | Full-text accessible  | Availability restricted   |

## 2.2. Search Results

The study included 74 articles published from 2009 to 2023 (May). Researchers' focus has continuously increased in the past few years on developing novel BRBs to enhance their performance. Figure 4 displays that during the initial two years of the selected duration, two articles were published every year on this topic. From 2011, the number of studies increased, reaching a maximum of 16 articles published in 2017. Subsequently, there was a moderate tendency in the number of publications in the domain of developing innovative BRBs, with an average of approximately 5 articles published annually.

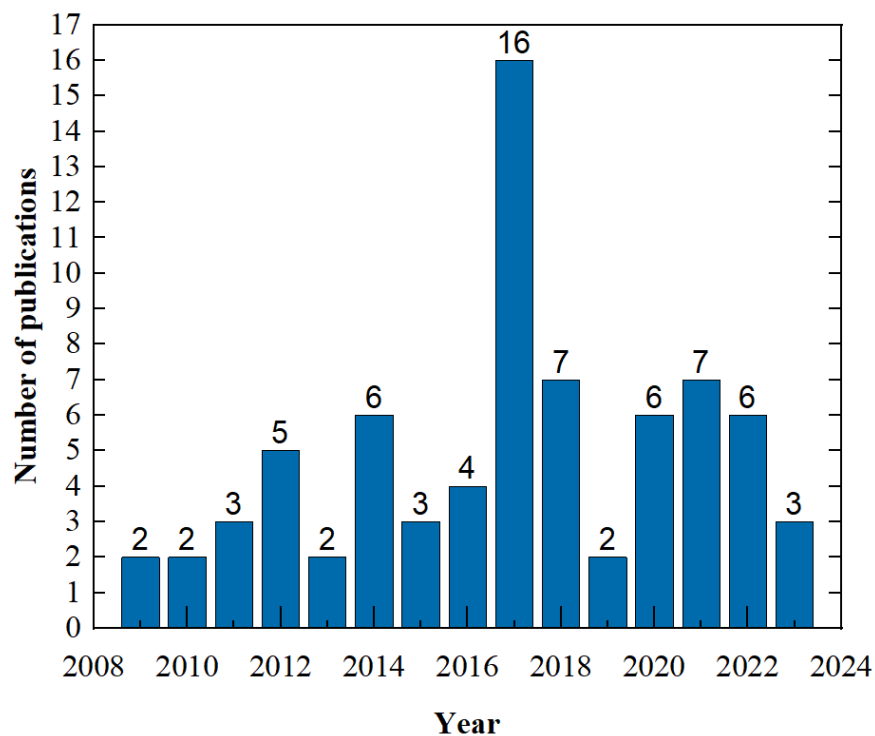


**Figure 4.** Distribution of articles per year.

Figure 5 illustrates the journals of the selected articles, the journal “Engineering Structures” (22) exhibited the highest publication rate, followed by “Journal of Constructional Steel Research” which contained fifteen articles. In addition, five articles were published in

“Journal of Structural Engineering” and “Earthquake Engineering and Structural Dynamics” and among the remaining journals, each has one to four articles.

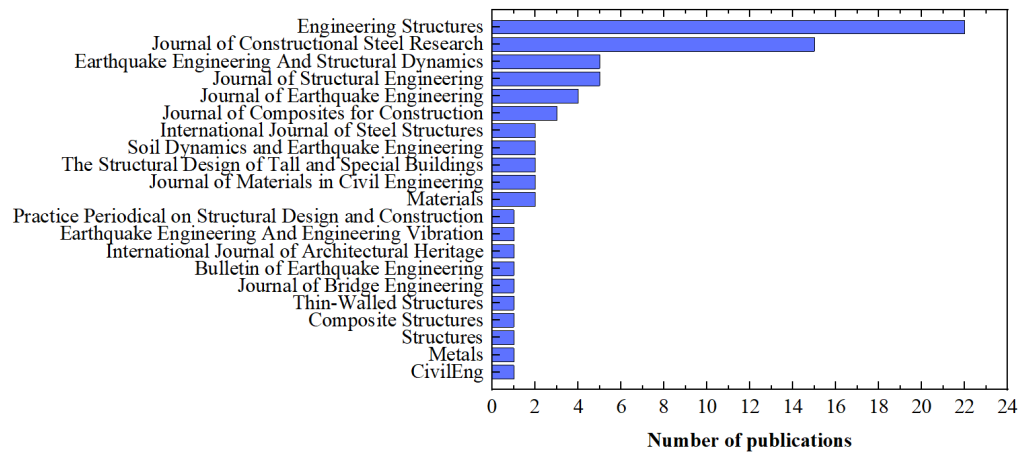


**Figure 5.** List of journals featuring selected articles.

Figure 6 demonstrates the geographical distribution of the selected publications based on the country of the first author’s institute. The authors of 74 articles belonged to 14 countries (China, USA, Iran, Japan, Taiwan, South Korea, India, Spain, United Arab Emirates, Argentina, Canada, Italy, Portugal, and the Turkey). Research institutes from China published most of the articles (50%), followed by the USA (11%), Iran (10%), and Japan (7%), and from the remaining countries each contributed (4%) to (1%) to the overall research output.

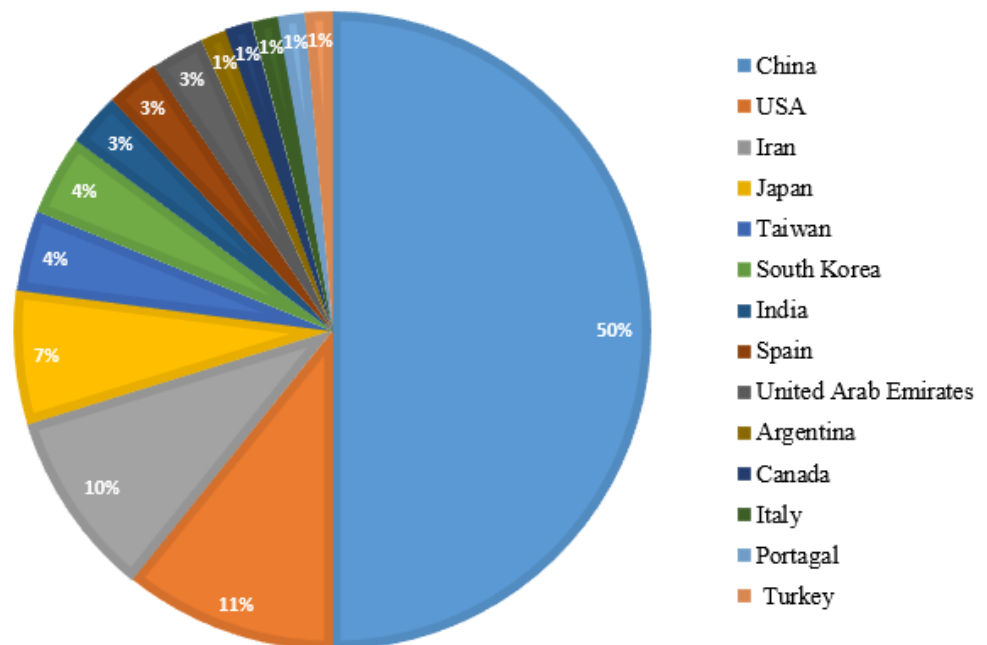


**Figure 6.** Geographical distribution of articles.

### 3. Discussion

Based on the selected articles, several types of BRBs have been developed and examined over the years. The BRBs can be categorized mainly according to the material properties of their components (core, un-bonding layer, infilled material, and external restraining component) and the shapes adopted to produce the braces as shown in Figure 7.

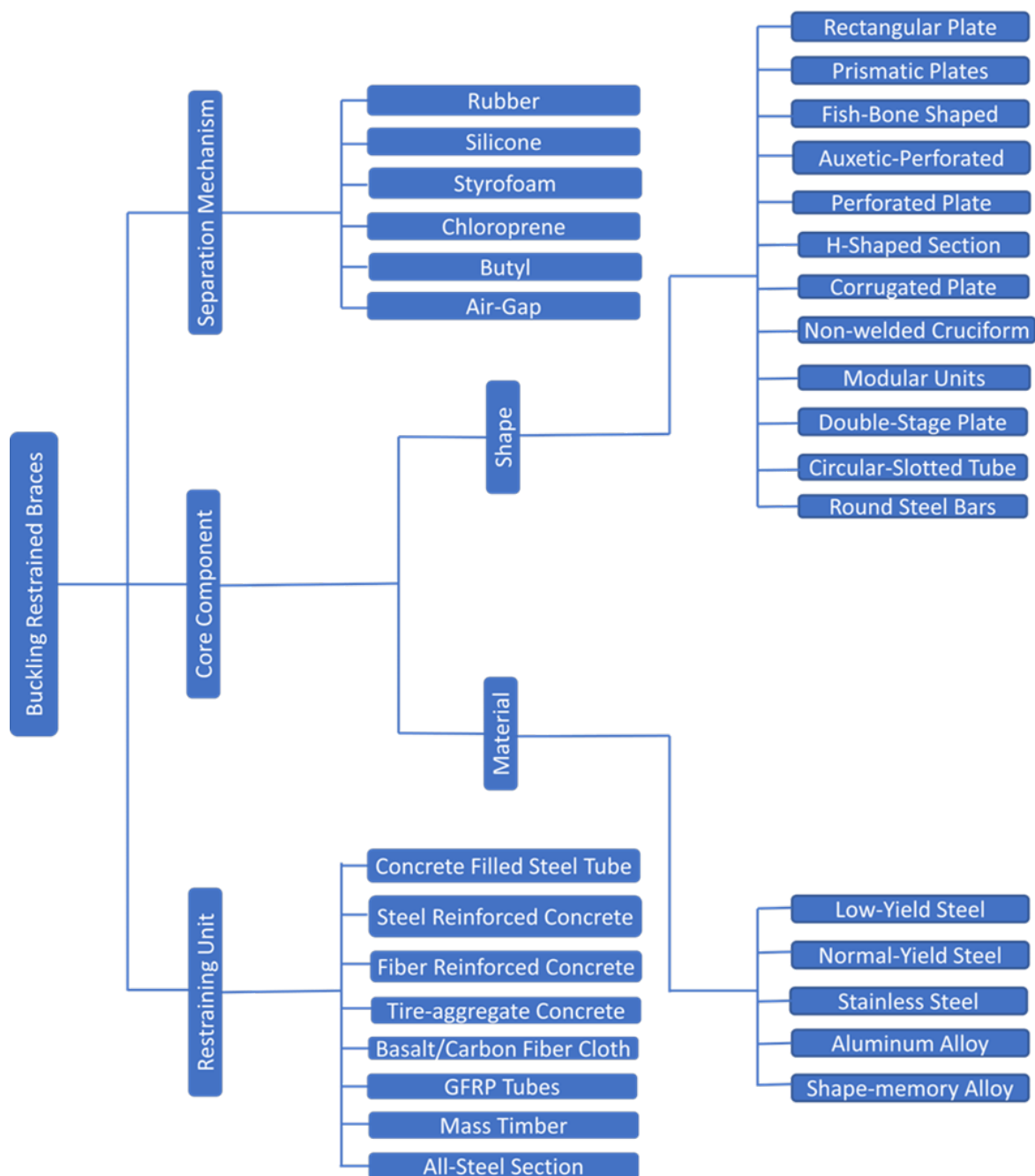


**Figure 7.** Types of BRBs based on components.

### 3.1. Studies Based on Core Component Materials of BRBs

The brace core is considered the most important component of BRBs because it is directly connected to the main structure and designed to withstand all the applied axial loads [63]. The material selected for the core component has an important impact on the performance of BRBs. To meet the requirement of energy dissipation capacities and hysteretic properties under intense earthquakes, the material should have adequate ductility, stiffness, and strength. Carbon steel, also known as structural steel with a yield strength of about 235 MPa, is mostly used in steel structures because of being relatively economical and having better toughness, strength, and welding properties. In the past, according to a comprehensive study about applications of BRBs [41], most of the researchers used this material with different designations ASTM A36 [64], JIS SS400 [65], and GB Q235B [66]

to manufacture the core components. The present study is focused on including recent findings that explore the utilization of novel materials to improve the performance of BRBs.

The aluminum alloy consists primarily of aluminum, with additional elements added to improve strength, such as iron, silicon, copper, magnesium, manganese, and zinc. Despite the exceptional qualities, such as lightweight, high strength-to-weight ratio, good corrosion resistance, durability, recyclable characteristics, high strength analogous to carbon steel, easy formability (e.g., extrusion), and long history of use in building structures as non-structural components, aluminum alloys still only make up a small percentage of studies related to BRBs [67]. Low-yield-point steel is a type of steel that possesses a yield strength of less than 235 MPa and the development of this steel was started by Japan as a material with excellent hysteretic properties that provide higher ductility, efficient energy dissipation, and shock absorption [68]. The core components of BRBs have also been constructed using low yield point (LYP) steel due to its exceptional properties, either as the sole material or in combination with other grades.

Stainless steel is an alloy of steel that contains a minimum of 10.5% chromium by weight, as well as other elements like nickel, manganese, molybdenum, aluminum, or titanium. The incorporation of these chemical constituents enhances the properties of the material to suit various applications and operating conditions. In recent years, the use of stainless steel in load-bearing structural applications has grown significantly, primarily due to its excellent strength, stiffness, and durability characteristics, as well as its low maintenance requirements [69–72]. Stainless steel plates have been used to form hybrid cores of BRBs and most recently, Al-Sadoon [73] proposed a grout-filled BRB using a stainless-steel bar as the replaceable fuse.

Shape memory alloys (SMAs) are a type of smart metallic material with the capability to retrieve prominent deformations through shape-changing sequences, including shape memory effect (SME) and super elasticity (SE). SME involves shape repossession after deformation in the martensitic stage upon heating to a specific temperature level, while SE is termed as unloading-dependent shape recovery after deformation in the austenitic phase. These characteristics have directed the development of various smart systems for use in several industries, incorporating aerospace, biomedical, civil engineering, and oil-gas sector [57]. Vibration control and energy damping needs can be effectively addressed through the promising implementation of SMAs. In 2020, Ghowsi et al. [74] developed a novel BRB using Fe-based shape memory alloy plates as the yielding core component. Fe-based SMAs are based on iron (Fe) as the primary constituent and exhibit a shape memory effect similar to other SMAs, enabling them to return to their original shape under certain conditions such as temperature or stress. Compared to other SMAs, Fe-based SMAs have several advantages, including low cost, abundance of raw materials, and high magnetic properties, making them suitable for various applications.

Ingot iron contains less than 0.1% of carbon content and is relatively ductile and soft as compared to carbon steel. Recently, Tao et al. [75] used this material to develop a new type of BRB and explored its suitability for low-cycle fatigue behavior. A summary of distinctive BRBs manufactured with these materials is presented in Table 2.

**Table 2.** Summary of the studies based on cores material.

| Reference       | Material Grade | Number of Specimens | Purpose of Study  | Compressive Strength Adjustment Factor ( $\beta$ ) |
|-----------------|----------------|---------------------|---|--|
| Shi et al. [76] | Q195           | 6                   | Development of Q195 low-yield point steel BRBs with the in-line cross-section | 1.08   |

Table 2. Cont.

| Reference             | Material Grade   | Number of Specimens | Purpose of Study   | Compressive Strength Adjustment Factor ( $\beta$ ) |
|-----------------------|--|---------------------|--|--|
| Huang et al. [77]     | Q195   | 6                   | Devising all-steel BRBs using Q195 low-yield core and Q345 for restraining unit                                | 1.62   |
| Wang et al. [78]      | SLY100   | 4                   | Development of BRB's finite element models using low-yield steel constitutive model                            | 1.23   |
| Ghowsi et al. [74]    | FeSMA  | 5                   | Development of new BRBs using iron-based shape memory alloy for core components and steel for restraining unit | 1.18   |
| Qiu et al. [79]       | FeSMA  | 3                   | Seismic performance analysis of iron-based shape memory alloy (FeSMA) BRBs                                     | 1.2  |
| Al-Sadoon et al. [80] | AISI 12L14 carbon steel<br>AISI 304 stainless steel<br>AISI 4140<br>chromemolybdenum<br>high-tensile steel | 3                   | Development of new BRBs for retrofitting of RC frames employing three distinctive materials bars cores         | 1.46   |
| Al-Sadoon et al. [73] | SS 304   | 6                   | Development of novel grout-filled BRBs with stainless steel bar core component                                 | 1.76   |
| Lanning et al. [81]   | 304/304L   | 6                   | Testing of BRBs with stainless steel cores for installing on long-span near-fault bridges                      | 1.39   |
| Tao et al. [75]       | Ingot-iron   | 8                   | Development of ingot-iron-core BRBs to explore their suitability as high-elongation material                   | 1.51   |
| Cigdem et al. [82]    | A508   | 4                   | Development of concrete-filled Aluminum-BRBs   | 1.76   |
| Usami et al. [67]     | A508   | 18                  | Development of all-aluminum alloy BRBs   | 1.11   |
| Wang et al. [83]      | HS63   | 10                  | Development of all-aluminum BRBs using a new aluminum alloy-HS63S-T5 for the core component                    | 1.04   |
| Proença et al. [84]   | 6082-AN350/120   | 1                   | Numerical simulation of Aluminum BRBs for seismic retrofitting of pilots' buildings                            | 1.17   |

Table 2. Cont.

| Reference              | Material Grade                          | Number of Specimens | Purpose of Study  | Compressive Strength Adjustment Factor ( $\beta$ ) |
|------------------------|---|---------------------|---|--|
| Tabatabaei et al. [85] | DIN 17100                               | 2                   | Development of Reduced-length BRBs using German standard ST 37-2 steel for cores  | 1.25   |
| Xu et al. [86]         | Q235<br>LYP225<br>EN 1.4301             | 7                   | Development of double-tube BRBs with different material cores   | 1.08   |
| Hoveidae et al. [87]   | G50<br>LYP100<br>SS 304L                | 7                   | Development of novel all-steel BRBs with a hybrid core made of three different materials                                    | 1.16   |
| Dehghani et al. [88]   | CSA G40.21-350WT                        | 12                  | Development of a full-scale BRB system using Canadian standard category 4 steel   | 1.47   |
| Wang et al. [89]       | SM400A                                  | 12                  | Improvement of low-cycle fatigue response of high-performance mild steel BRBs by employing Toe-finished method              | 1.14   |
| Seker et al. [90]      | ASTM A500 Gr. B                         | 3                   | Development of all-steel tube-in-tube buckling controlled brace   | 1.10   |
| Kim et al. [91]        | SS400<br>HYUNDAI-STEEL                  | 3                   | Development of Concrete-filled and hollow steel tube BRBs using SS400 and SM490 for cores and external units, respectively, | 1.20   |
| Atlayan et al. [92]    | ASTM A36<br>LYP100<br>HPS-70W           | 3                   | Development of hybrid-core BRBs for multi-level hazards   | 1.05   |
| Wang et al. [93]       | Q235<br>1860-grade<br>high-strength wir | 1                   | Development of innovative BRB with gap-supported tendon protection  | 1.19   |
| Sitler et al. [94]     | LY225<br>SA440B                         | 1                   | Development of multistage mortar-filled BRBs using two cores of different materials   | 1.06   |

### 3.2. Studies Based on Core Component Shapes of BRBs

The core component is designed to concentrate the inelastic deformation in the central region to keep both ends in elastic range and to ensure this phenomenon, the yielding zone is shaped like a tensile coupon or small holes are made to reduce the area. In the past, various forms of core components have been proposed and investigated as shown in Figure 8.

The rectangular-shaped core was used in the first practically implemented BRB and is still the common type because of its ability to provide a desirable hysteretic response and simpler and welding-free manufacturing. In 2010, Mirtaheeri et al. [95] used rectangular plates as core components to conduct an analytical and experimental study on concrete-filled BRBs. This study was mainly carried out to analyze the effect of core length on the overall behavior of braces and the core plates were developed with different connections (pinned and stiffened end-plate) to install in the test setup as shown in Figure 8a. The experimental work was started on a 140 cm long trial specimen to insight the possible deficiencies and subsequently, four braces of distinctive lengths were fabricated with improved configurations to conduct the main tests. All braces showed stable responses without any significant drop in compressive and tensile strengths and stiffness was found inversely to core length because the specimen with minimum length showed the highest stiffness.

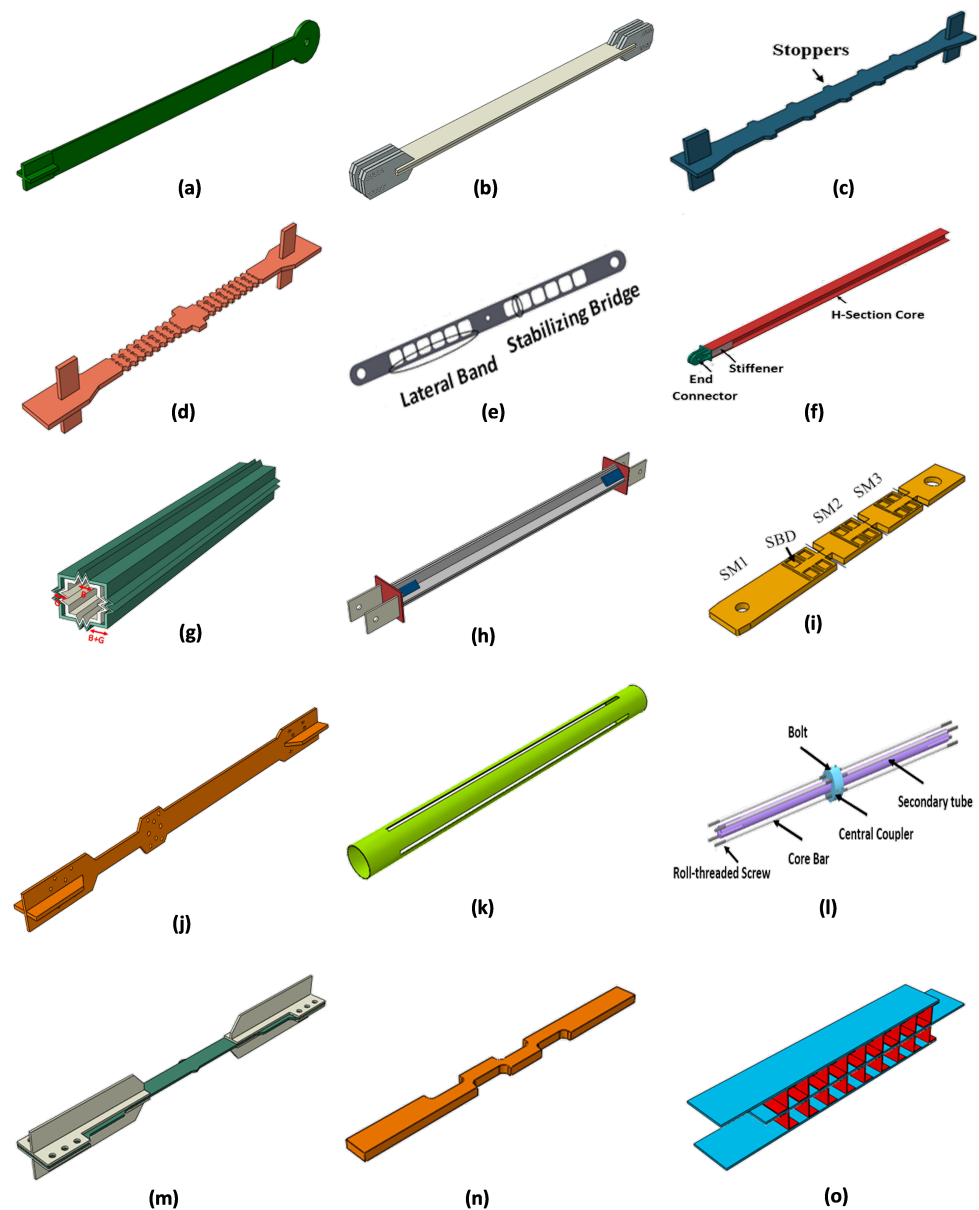


**Figure 8.** Shapes of cores introduced to develop new BRBs [95–109].

In another study, Xu et al. [96] introduced BRBs with prismatic steel plates as core components to reduce manufacturing costs and avoid waste of material. The core plates were straight throughout their length without any cuts or holes and connection plates were

welded perpendicularly at core ends to attach the braces with gusset plates as shown in Figure 8b. A total of four specimens were tested, in which two braces contained single plate core components while the other two were fabricated using dual plates with identical thicknesses of 25 mm. The results revealed that there was no brace instability, rupture, or failure in the connection region up to loading equivalent to 2% story drift and the load-displacement curves showed stable response with satisfactory increasing stiffness.

Modifying the rectangular plates, Jia et al. [97] introduced a fish-bone-shaped core component to fabricate an all-steel BRB with smoothed dismountable requirements. Multiple stoppers on both sides of core components were machined to maximize the deformation capacity of the proposed BRB by developing several necks in the core plates before the rupture as shown in Figure 8c. Experimental and numerical studies were conducted to investigate different design parameters and configurations. The study found improved seismic performance for newly developed fishbone-shaped BRBs as compared to conventional BRBs and a maximum value of 20.6 was recommended for the width-to-thickness ratio of the core component to avoid pre-mature local buckling. Auxetic metamaterials have been increasingly studied for civil engineering applications due to their distinctive deformation attributes and mechanical characteristics like appropriate energy dissipation capability, enhanced shear, and fracture resistances. Zhang et al. [98] manufactured a small-scale all-steel BRB with a perforated core as shown in Figure 8d, having a negative Poisson ratio to delve into the hysteretic response of auxetic metamaterials under cyclic loading. Experimental and numerical studies were conducted to mainly investigate the effects of porosity, auxetic unit cell, and section weakening rate. The newly-developed negative Poisson ratio BRB showed a stable hysteretic response and a comparison of its performance with conventional perforated core BRB having a positive Poisson ratio demonstrated that the usage of auxetic metamaterials can be advantageous for the development of damping devices to mitigate the seismic effects.

Cahís et al. [99] also introduced a new perforated-core all-steel BRB that not only lessens the weight but also facilitates the post-earthquake examination. The usually adopted dog-bone-shaped core in this new BRB was replaced with a rectangular cross-section perimeter that has a constant size, and its yielding part was divided into two lateral bands which were linked by stabilizing bridges as shown in Figure 8e. The lateral bands in the design of the new core component were intended to yield under axial forces similar to conventional BRBs, but stabilizing bridges were proposed to maintain their elasticity. Two specimens with different geometries of core elements were tested up to failure under different loading patterns. The radius of the lateral band connections was the primary distinguishing factor between the two geometries. According to the experimental results, the specimen with a smaller radius, even though it provided a longer yielding length with a constant cross-section, resulted in reduced dissipation capacity and a smaller distance between the stabilizing bridges. This specimen also experienced gradual compression capacity reduction due to local buckling as compared to the larger radius specimen which displayed a consistent response.

BRBs with H-section core components can withstand large axial loads and are cost-effective because H-shaped members are readily available. Alemayehu et al. [100] presented a NOVEL all-steel BRB, comprised of an H-section core component as shown in Figure 8f which was enclosed in a square tube, having unique properties with minimum construction noise, CO<sub>2</sub> emission, vibration, labor efforts, and enhanced energy dissipation capacity. Experimental and FE parametric studies were conducted on full-scale brace specimens and subassembly under displacement-based cyclic loading according to the American Institute of Steel Construction seismic provision (AISC) [110]. Two failure patterns (global buckling and flange buckling of core components) were observed as most predominant, and it was found the proposed BRB can provide a stable hysteretic response till the end of applied loading with a minimum flange slenderness ratio of 5.06.

Corrugated plates are capable of showing high buckling resistance under in-plane loads and enhanced out-of-plane stiffness because of their geometric properties.

Jamkhaneh et al. [101] proposed a new all-steel BRB with a corrugated-edges core as shown in Figure 8g and exterior components without including the welding process to enhance the plastic deformation and energy dissipation capabilities. FEM models under cyclic loadings were developed to validate the laboratory specimens and analyze the effects of gap distance between the core and external sheets and the sizes of brace sections. A 10 mm value size gap was found most appropriate for the distance between the components and the results showed that the installation of corrugated-edges BRBs can increase the ductility and performance level of high-rise structures.

BRBs with cruciform-shaped core components facilitate brace and gusset plate connection. A welded cruciform core component can affect the low-cycle fatigue properties of braces due to significant residual deformations resulting from high-temperature welding. To diminish the initial geometric imperfections of core components and improve low-cycle fatigue response, Zhao et al. [102] introduced a novel angle all-steel BRB. As illustrated in Figure 8h, the core component was fabricated by combing four steel angles with eight stiffening plates at the ends to produce a cruciform shape without welding in the yielding section. Hing connectors were welded at both ends and the restraining component was formed by combing two angles through longitudinal welding. All seven tested specimens exhibited stable hysteretic performance and were found feasible to employ as seismic dampers. The authors recommended that the projected parts of the core component should be might in an elastic state to avoid compression–flexure failure.

To facilitate the transportation, installation, maintenance, and replacement of BRBs parts, Piedrafita et al. [103] developed a novel approach using a modular steel-yielding core component. This design allows for the use of smaller units and enables adjustments to the yielding load and plastic deformation based on specific design requirements. The concept of Modular BRB was devised from the idea of connecting the buckling self-stability of the small-scale steel energy dissipation devices. As shown in Figure 8i, the core consisted of several seriated modules which were connected through the pins to permit the transmission of axial force from one module to the other and each module contained several Shear Basic Dissipation Units (SBDUs) to ensure the yielding by shear. Experiments and FEM simulations were performed on full-scale specimens under displacement-based cyclic loadings to analyze the yielding force and displacements. The results demonstrated balanced hysteretic responses and the axial force of the whole specimen was found to be dependent on the number of Shear Basic Dissipation Units (SBDUs) for each module.

To make the BRBs adaptive to different earthquake actions, Sun et al. [104] introduced a double-stage yielding BRB with the idea that the brace will partially yield under frequent and minor earthquakes and also withstand large axial loads to limit structural damage in the case of rare earthquakes. The core component of this brace was comprised of two plates, one small and one large plate, which were combined in series as shown in Figure 8j. The constitution of the double-yield BRB core component was analogous to the traditional BRBs and could be considered a tandem formation of two conventional all-steel BRBs having different sizes. In addition to small and large plates, the core component also contained a stopper mechanism to activate the function of the large part after the maximum deformation capacity of the small one under rare seismic action. Two ribs were also welded at both ends of the core component to ensure the inelastic deformation in reduced sections. Quasi-static tests on three specimens were performed to analyze the influence of varying lengths for the core component plates. All specimens demonstrated ductile and stable hysteretic performance and the ratios of maximum compressive–tensile forces remained within the range of 1.3 as recommended by AISC [110].

Dongbin et al. [105] proposed novel three-steel tubes BRBs to ease the fabrication process and enhance energy dissipation capacity. In this BRB, three circular tubes of different diameters were used and placed as inner, middle, and outer tubes. The middle tube with slotted holes was supposed to be the core component which is shown in Figure 8k, and the inner and outer tubes performed the restraining unit function to impede the core's compressive buckling. The same air gap of 1.5 mm was employed between all

tubes without laying any debonding material. The inner and middle tubes were used as one part, while the outer tube was divided into two sections of identical lengths and all three tubes were connected through spot-welding at mid-span to keep them at exact positions. Five specimens with distinct sizes and the number of holes in the core components were tested under quasi-cyclic loading to analyze the performance of the proposed braces. Based on the results, the composition of braces was found effective and reasonable, and all specimens produced balanced and saturated hysteretic curves. The brace exhibited excellent performance in terms of low-cycle fatigue response and deformation capacity with  $2 \times 2$  slotted holes and a 0.2 opening-hole ratio of the core component.

In comparison to steel plates and tubes, round steel bar cores used in BRBs provide a significant advantage due to the ability to connect bar ends to the structural members using screw joints. Recently, Zhang et al. [106] proposed a novel all-steel BRB by employing four round steel bars as core components to enhance the reasonable strengths of braces and reduce their manufacturing cost. The core part contained eight bars with roll-threaded screw ends, which were connected to the central coupler through screws as shown in Figure 8l. Two restraining members, known as primary and secondary tubes were utilized to restrict the buckling of braces. The primary tubes were mainly designed to restrict the buckling of core bars, whereas the secondary tubes were enacted to restrain the primary tubes from buckling through spacers. Three specimens with varying spacings of spacers were manufactured and tested to assess the structural performance of the proposed braces. Based on the comparison of hysteretic curves, two specimens with spacers spacing of 275 mm and 415 mm, respectively, exhibited stable and satisfied hysteretic behaviors, while the third specimen with a maximum spacing of 824 mm could not perform well due to the buckling of primary tubes.

To remove the impact of welding on the low-cycle fatigue performance, Xie [107] developed a weld-free sort of all-steel BRB. The whole BRB was designed without a single weld and the core component was fabricated from a steel plate through line cutting. Two T-shaped sections manufactured from H-shaped steel were fastened with high-strength bolts on each end to increase the stiffness of connection zones as shown in Figure 8m. The stoppers in the center of cores were created as a convex arc-shaped boundary to produce a steady shift of section. Under various strain amplitudes, three welded and three weld-free specimens were tested, and their hysteretic behavior and low-cycle fatigue performance were examined. The test findings showed that the weld-free specimens have substantially higher ductility and cumulative plastic deformation than the welded ones, which are much closer to the material capacity's performance.

Due to their excellent seismic performance, miniature BRBs are frequently utilized as energy-dissipating dampers in precast concrete and steel beam-to-column connections. Gu [108] proposed a novel all-steel corrugated MBRB (CMRB) by employing corrugated core components surrounded by circular tube restraining units. In order to increase ductility and enable the CMRB to be shorter than traditional MBRBs, various D-shaped cuttings, also known as D-cuts, were designed on the core elements as shown in Figure 8n. This design requires a lower installation area for the beam-to-column connections and to explore the impacts of section spacing-to-D-cut cross-section height ratio and slenderness ratio on seismic performance, six specimens were constructed and tested under cyclic loading. All tested specimens exhibited favorable cumulative deformation capacity and the seismic performance of the proposed CMRB was observed to be influenced significantly by the slenderness ratio ( $\lambda$ ) and the ratio of segment spacing to D-cut cross-section height ( $D$ ).

Jamkhaneh [109] introduced a novel all-steel BRB consisting of mainly three parallel plates which were combined together with Z-shaped sections as shown in Figure 8o. The employed plates having adequate strength and stiffness, were positioned with respect to the weak axis, spreading the force among them. The position and depth of the plates inside the system were adjustable and the system's resistance, stiffness, and ductility could be changed by adjusting the quantity, thickness, and heights of the plates utilized. The plastic joints were created for the top and bottom of every plate and were attached to

the corresponding plates, and this mechanism resulted in energy absorption in a targeted manner. Initially, the cyclic response of the proposed BRB was inspected through finite-element modeling and then 5, 10, and 15-story steel buildings were numerically designed to examine the performances through nonlinear dynamic and static analyses. The results demonstrated that the newly developed BRBs were able to obtain the performance level of structural-life safety.

### 3.3. Studies Based on Debonding Mechanism of BRBs

The separation mechanism between the core and buckling-restraining components has a significant influence on the performance of BRBs. It generates a space for the core to expand transversely under the compressive loads and stops shear stress transfer. This debonding process needs a thin film-like material and a small gap can be placed between the core and the restraining unit. In the past, different materials have been investigated for this purpose.

Tsai et al. [111] developed 13 full-scale BRBs and performed experiments to analyze the effectiveness of four debonding materials shown in Figure 9, (chloroprene rubber (CR), silicone rubber sheet (SR), rubber sheet (R), and high-density Styrofoam sheet (HS)) for reducing the variance between the maximum compressive and tensile strengths. The influences of the ratio between yielding length and whole specimen work-point to work-point length on the axial stiffness of the braces and design story drift were also investigated. All tested specimens unveiled satisfied hysteretic performances and results indicated that the chloroprene rubber (CR) having self-adhesive properties was found most convenient for placing on the core components and very efficient in minimizing the variances between the maximum compressive and tensile values in the hysteretic curves.

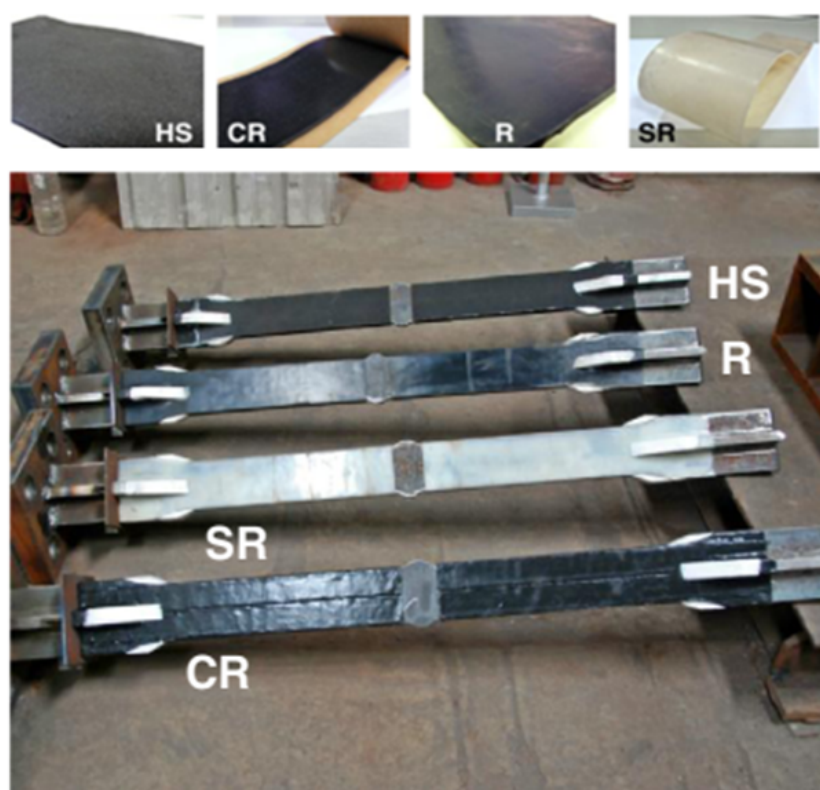


**Figure 9.** Placement of four different debonding materials on cores. (Reprinted with permission from Ref. [111]. Copyright 2014 John Wiley and Sons.)

Chen et al. [112] developed all-steel BRBs by employing a pure gap and a 1-mm thick layer of butyl rubber between the core components and exterior restraining units as shown in Figure 10 and conducted an experimental study on seven specimens to analyze the

variances in the low-cycle fatigue performances. The results demonstrated that all specimens were able to dissipate adequate energy and sustain collective plastic deformations 1000 times more than the yield strain. However, the absence of unbonding materials created jamming and gradually increased the friction forces between the core and restraining components, which ultimately led to a substantially higher compression strength adjustment factor. In addition to this, the jamming and friction forces developed non-uniform residual deformations and it was recommended to install unbonding layers to achieve better performance of all-steel BRBs.

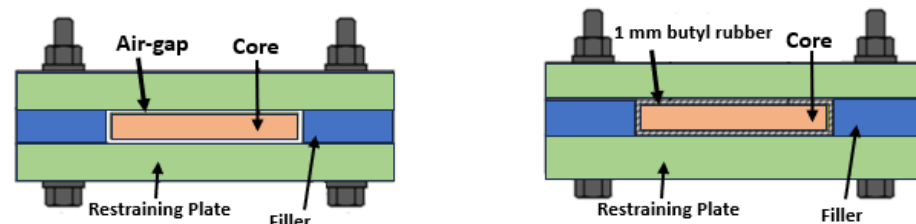


**Figure 10.** Composition of all-steel BRB by placing air-gap and butyl rubber for debonding process [112].

Chou et al. [113] proposed conventional concrete-filled BRBs by employing a pure air gap instead of unbonding material between the core component and exterior restraining units and performed four sub-assembly experiments to examine the inelastic deformations. The developed BRB contained a dog-bone-shaped core component that was sandwiched between two identical restraining units. Each restraining component was manufactured by welding a channel section to a flat plate and filled with 28-days concrete. Along with experimental tests, a FEM parametric study on 18 specimens was conducted and found that the ratio between maximum compressive and tensile strengths remained in the range of 1.1–1.5 and mainly concluded that the replacement of unbonding material with air space would not affect the cyclic performance of the proposed BRBs.

In another study, Wu et al. [114] also developed all-steel BRBs without implying any debonding materials on the surfaces of core parts and conducted detailed experimental and finite element investigations to examine the high-mode buckling process of core components. The proposed cores and restraining units were bolted through shim spacers as shown in Figure 11 and a dust-remover WD-40 lubricant was sprayed on the inner sides of restraining components and the whole surface of core parts. Test results revealed that the developed braces sustained large cyclic strains and underwent cumulative plastic deformations over 400 times the yield strain values. Through this study, it was confirmed that the high-mode buckling wavelength of core components was dependent on their thickness sizes and the patterns of loading protocols.

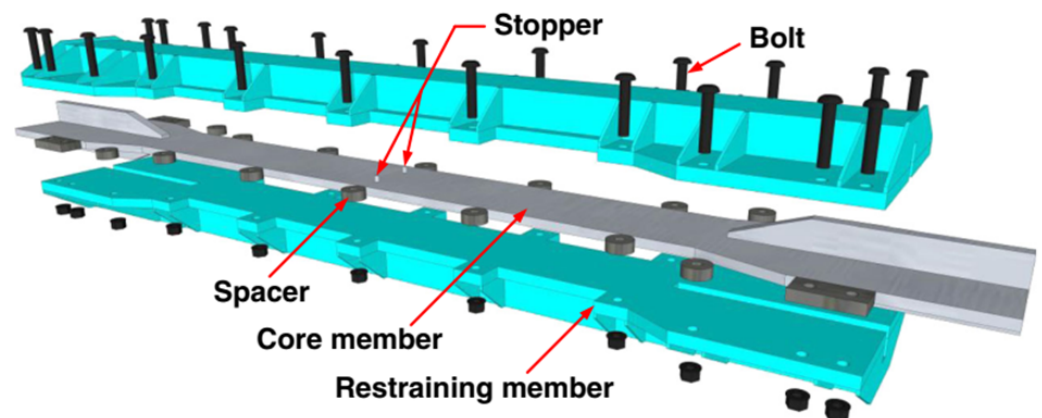


**Figure 11.** Composition of BRB with shim spacers. (Reprinted with permission from Ref. [114]. Copyright 2013 John Wiley and Sons.)

The thickness of applied unbonding materials is also considered significant for the design of BRBs. Palazzo et al. [115] proposed a low-cost durable buckling restrained using easy-to-find construction materials. The developed device comprised a slender solid steel bar core component and a high-strength mortar-filled circular steel tube as a restraining system. A three-layered periphery was applied to limit the transfer of shear stresses from the core component to the surrounding mortar and ensure proper sliding between them. Firstly, the core component was coated and lubricated with Teflon and grease, respectively, and then wrapped with a 1.7 mm thick rubber. The tested braces showed a stable hysteretic response and it was suggested that a too-thin debonding layer would inhibit the core component from expanding laterally, and a thick layer could permit enlarged local buckling which ultimately caused a reduction in the fatigue life of braces.

To analyze the lateral thrust applied from core components on restraining units, Genna et al. [116,117] presented bolted steel BRBs by employing a synthetic general-purpose paste (BERULUB PAL 3) for debonding process and reducing friction. The incorporation of a solid lubricant, specifically polytetrafluoroethylene, into the material resulted in a significant decrease in the friction coefficient. The configured BRB was developed with a rectangular steel plate core, which is encased and restrained by two bolted C-shaped steel struts. Six reduced-scale specimens with two different cross-sections of cores and three altered core-restraining gaps were tested inside the INSTRON 1274/8500 apparatus under displacement-controlled loading specified by the AISC standards (AISC 2005). In continuation of this study, engineering analytical expressions of the thrust were developed by considering the air gap between the core and restraining struts. In conclusion, it was found that accurate prediction of the total thrust for these BRBs was challenging due to the discontinuous relationship between its value and the loading history. It was stated that the real behavior of these BRBs and the developed analytical expressions were conditional for a sufficiently small casing-core gap. If the gaps become excessively large, the BRBs lose their ability to dissipate energy in compression, leading to notable geometrical effects.

### 3.4. Studies Based on Restraining Units of BRBs

The restraining encasings have functions to stop the core component from buckling and ensure the same response in compression and tension of BRBs to dissipate more energy under earthquake actions as compared to ordinary steel braces. Therefore, the restraining element must have adequate stiffness and strength to substantiate the local stability as well as the global stability of the core component. In the case of conventional BRBs, the restraining component usually consists of a hollow steel section filled with traditional concrete or mortar, fiber-reinforced concrete, steel-reinforced concrete, and polymer-filled steel tubes.

#### 3.4.1. Conventional-Concrete BRBs

Zhang et al. [118] proposed an innovative spiral stirrup (SS-BRB) to reduce manufacturing costs and improve the service life of braces. The restraining unit of these novel braces was comprised of reinforced concrete with longitudinal steel bars and spiral stirrups to restrict the buckling of core components and enhance flexural capacity. A paper tube with a lubricated inner side was used as formwork to fill fine aggregate concrete and place the assembled cage of rebars as shown in Figure 12. Displacement-based cyclic tests were conducted to investigate the feasibility of newly developed BRBs and examine their basic performance. The load-displacement response showed balanced hysteretic loops without any degradation in compressive and tensile strengths and proved this restraining system practical and reliable.

Gheidi et al. [119] organized a series of experiments to discover different infilled materials to prevent the buckling of core components in BRBs. Three infill materials compacted aggregate, lean/lightweight concrete, and normal concrete were included with a perception to decrease the overall weight of braces and eliminate debonding agents. The results revealed that the compacted aggregate (non-cohesive) material was not feasible to limit the

buckling of the core component, which caused a prompt reduction in compressive strength. The specimens with lean concrete showed a 30% reduction in the efficiency of braces due to the crushing of concrete and local buckling failure of core components. Normal concrete was found to be the most efficient infilling material because the braces with this material performed stable hysteretic response with enhanced energy dissipation capacity.

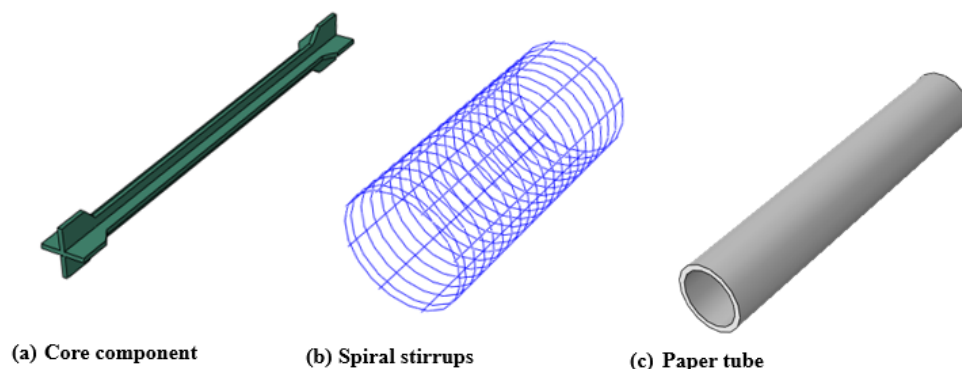


Figure 12. Components of spiral stirrups BRBs: (a) steel core (b) spiral stirrups (c) paper tube [118].

Takeuchi et al. [120] developed mortar-filled conventional BRBs with different sectional shapes of exterior restrainers and conducted cyclic loading experiments with varying mortar thicknesses. This study also proposed an approach to prevent the in-plane local-buckling failure of the core component. Rectangular and circular-shaped steel tubes were employed as restraining components with distinctive thicknesses, and it was observed that mortar thickness affected buckling failure initiation and local buckling failure delayed as mortar thickness increased. The local-buckling failure of specimens having circular-shaped restraint did not occur until the plastic strain amplitude of the core component reached 3% even with larger values of diameter-to-thickness ratios, while the braces with rectangular tubes having width-to-thickness ratios of 65 and 76 showed local-buckling failures.

Esfandiari et al. [121] developed fiber-reinforced concrete BRBs and conducted a series of experiments on six samples by using only concrete as a restraining unit. Initially, compressive, and tensile strengths tests were carried out on concrete cubes containing polypropylene, macrostructure, and hybrid (combination of polypropylene and steel fibers) fibers to determine their optimum amount and the results indicated that the non-fibrous samples showed lower compressive and tensile strengths as compared to polypropylene and hybrid fibers cubes. The samples of used fiber are shown in Figure 13 and the test matrix was categorized into three groups non-fibrous, polypropylene, and hybrid fibers BRBs according to the composition of fibers in the restraining component. Experiments were performed under displacement-based cyclic loading and the braces with hybrid fibers concrete were able to bear the maximum number of loading cycles and also performed better as compared to other groups in terms of energy absorption capacity, structural ductility, and undergoing higher compressive and tensile loads.

Alemayehu et al. [122] proposed a tube-in-tube BRB using a quick-hardening and lightweight polymer as filling material between core and restrainer components as displayed in Figure 14. The tube-in-tube composition reduces the required amount of infilling material and enables the braces to withstand large axial loads. The adopted polymer was able to fully solidify within 24 h at room temperature and had a density of  $1178 \text{ kg/m}^3$  in its hardened form equal to half of the mortar. Ten full-scale experiments of six circular and four-square-shaped specimens were conducted to investigate the buckling behavior and inelastic deformation capabilities of braces. The test results demonstrated that circular braces performed better, and the infilled material provided adequate resistance against buckling even with a small amount of its leakage in all experiments and future research was recommended to investigate the impact of this leakage and propose suitable remedies.



**Figure 13.** Samples of fibers used in Fiber-reinforced-concrete BRBs. (Reprinted with permission from Ref. [121]. Copyright 2018 Elsevier.)

With the aspiration to reduce the health hazards triggered by scrap tires, researchers have directed their attention toward the utilization of scrap tires in asphalt concrete, cementitious concrete, and soil embankments. These materials, referred to as tire-derived aggregates, offer energy dissipation and damping capabilities in different uses.

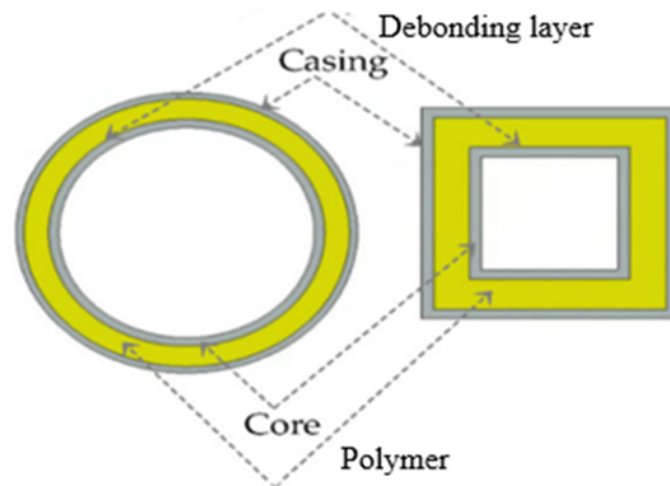


**Figure 14.** Configuration of Polymer-filled Tube-in-Tube BRB [122].

The concrete made from these recycled tires is commonly known as tire-derived aggregate concrete (TDA) or rubberized concrete. Recently, B. Pathan et al. [123] proposed novel BRBs using only tire-derived aggregate concrete as a restraining component without encompassing exterior steel tubes. To substitute mineral aggregates, Crumb rubber was produced through the mechanical shredding of recycled tires shown in Figure 15, and three specimens of BRBs were manufactured by using these aggregates. In addition to these, three conventional concrete-BRBs samples were also tested to compare their damping ratios, ductility, failure patterns, and energy dissipation capacities. All specimens were tested using a shake table in the structure's laboratory of California State University, Fresno, USA. From the results, it was found that TDA-BRBs provided additional damping and less energy dissipation as compared to conventional concrete braces and the authors advised using these braces exclusively in systems where damping is the main priority.



**Figure 15.** Samples of crumb rubber used in manufacturing of tire-aggregate-concrete BRBs [123].

### 3.4.2. All-Steel BRBs

All-steel BRBs differ from conventional BRBs with concrete-filled tubes in that all of the parts including the restraining unit are made of steel. These braces were developed to overcome the drawbacks of conventional concrete-filled BRBs.

To facilitate the post-earthquake investigation and reuse the buckling restraining units, Qu [46] proposed an innovative all-steel BRB containing substitutable steel angle fuses. The presented BRB consisted of three major assemblages: the inner telescopic buckling-restraining mechanism (BRM), the buckling constrained angle fuses, and the exterior BRM. Seven specimens were tested to examine the seismic response of the proposed braces by varying fuse design and material, unbonding material, and loading patterns. Based on the test results, the developed BRBs displayed consistent hysteretic response up to quite high fuse strain values. Expectedly, angle fuse fractures were found to be the specimens' failure mechanisms and the accumulated plastic deformation, and the compression strength adjustment parameters of all specimens satisfied the criteria set out by the current seismic design regulations for structural steel structures in the United States.

Ghowsi [124] devised a lightweight bolted all-steel BRB to facilitate the post-earthquake inspection of core elements. This novel solution prompted an in-depth exploration of its seismic performance, encompassing the analysis of axial strengths, displacement ductility, and energy dissipation capacities. The investigation encompassed diverse connection details, stopper positions, and debonding gaps, all aimed at enhancing the understanding of this innovative system's behavior. The main components of the proposed assembled-BRB consisted of a core component, a restraining unit, and end connection elements as shown in Figure 16. The central yielding region of the core component was composed of a rectangular cross-section and the consistent thickness of the cores continued to the transition and elastic segments. However, the cruciform layout was created by welding supplementary transverse stiffening plates on both sides of the core components to turn both transitional and end portions stronger. The restraining system was created by placing four steel angle sections back-to-back, fastening them together with high-strength (HS) bolts, and adding intermediary transverse stiffeners to the angle sections to increase their flexural rigidity. Six specimens were designed to perform sub-assembly experiments and all tests demonstrated excellent performance with stable energy dissipation up to 3% strain of cores.

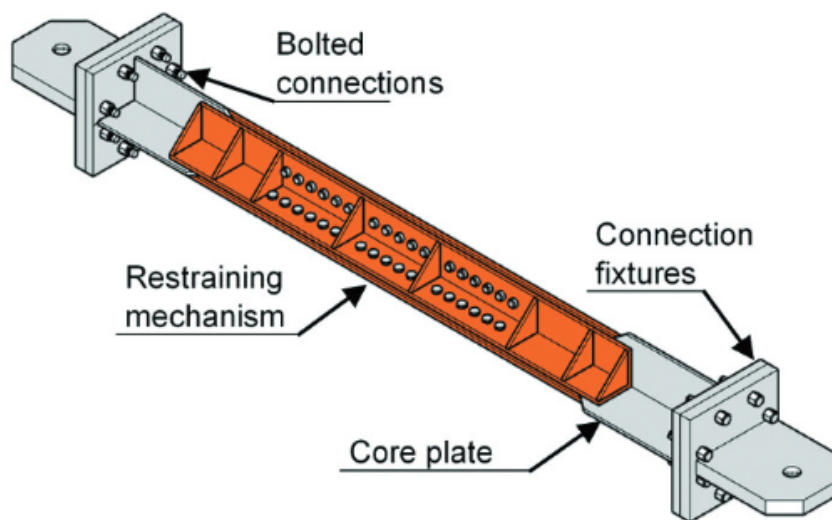


Figure 16. Assembly of angle restraining units all-steel BRB [125].

Guo et al. [126–128] introduced a core-separated all-steel BRB to enhance the efficiency of material utilization and investigated its hysteretic performance and buckling behavior experimentally and theoretically. This newly proposed core-separated all-steel BRB differs from traditional single-core BRB and contains two chord components that are combined together through continuous web-plates. These braces are lightweight as compared to conventional BRBs and can be fabricated and installed more conveniently in mega structures such as large-size BRBs. These studies also proposed a new method to design these braces based on normalized slenderness relating to the design procedure for axially compressed columns. Initially, a nonlinear finite element analysis was performed to investigate the hysteretic response of novel braces and acquire normalized critical slenderness values. Based on these slenderness values, four specimens were tested, and the results indicated that these core-separated braces can provide a balanced hysteretic response and have satisfactory energy dissipation ability with adequate stiffness of external restraining tubes.

Later, a new battened core-separated all-steel BRB was proposed by Guo et al. [125]. It was assumed that the battened BRBs can have significant advantages due to their assembly, in which two separate all-steel BRBs with individual welded encasing tubes were connected through longitudinally scattered battens as shown in Figure 17. This composition created a sectional cavity which increases the second moment of area and flexural stiffness of specimens due to outward spreading of the cross-section. Five specimens of battened braces were prepared to investigate their hysteretic response experimentally. To develop an integrated exterior restraining unit, sealing plates at both ends of specimens were welded with cornered steel battens and core stiffeners. The results revealed that the tested battened BRBs did not fulfill the energy dissipation requirements due to premature failure caused by the welding rupture of restraining units. Finally, the authors concluded that these braces can be considered only economical but not efficient in terms of hysteretic performance as compared to conventional BRBs.

To fulfill the requirement of bulk-size braces required for long-span spatial structures and mega-frame structures, Guo et al. [129,130] introduced a triple-truss-confined all-steel BRB. As shown in Figure 18, this novel triple-truss-confined all-steel BRB was fabricated by adding a series of rigid trusses around a conventional all-steel BRB to enhance the overall load-bearing capacity and flexural stiffness of the exterior restraining unit. Two 4.6 m long specimens with different thicknesses of the core component were designed and tested under standard-fatigue combined loading. The results indicated that both specimens attained excellent cumulative ductility and showed stable hysteretic responses and energy-absorption capacities. Although the novel triple-truss-confined braces (TTC-BRBs) fulfilled significant performance requirements for earthquake-resistant design of buildings

according to AISC seismic provisions [110] and the Chinese code GB50010 [131], the authors suggested imposing additional stiffeners at both ends to impede premature failure.

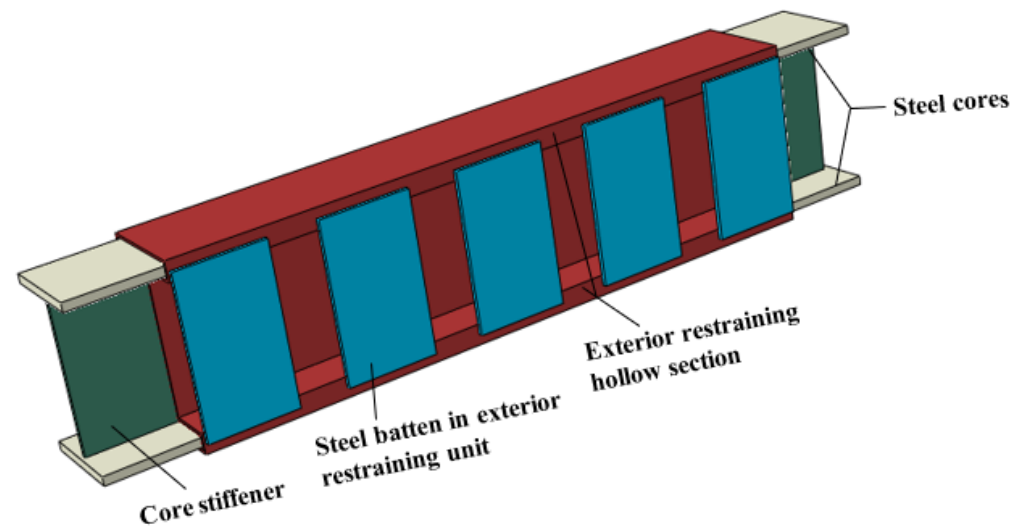


**Figure 17.** Assembly of batted core-separated all-steel BRB [125].

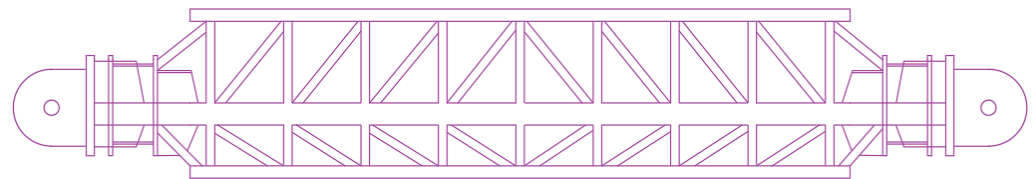


**Figure 18.** Tripple-truss-confined all-steel BRB [129].

Guo et al. [132,133] introduced an aesthetically appealing shuttle-shaped all-steel BRB to utilize in spatial and long-span structures. The developed shuttle-shaped BRB was comprised of three parts, a circular steel tube core component having a uniform cross-section, a steel-plate isolation system fabricated through welding of longitudinal and transverse annular plates, to fill the space between the core, and an exterior restraining unit made of shuttle-shaped thin-walled steel tube as shown in Figure 19. The core component was designed marginally longer than the exterior restraining unit to prevent the contracting of their end plates and to allow the shortening of the core under compression loading. In addition, four longitudinal stiffeners were welded around the ends of the core component to keep the connection section elastic and impede premature failure. Initially, elastic buckling analysis was conducted with pin-ended conditions based on the equilibrium method to establish the elastic buckling load calculation expression. Finally, the authors suggested a value of 2.5 for the restraining ratio of shuttle-shaped BRBs to acquire the maximum cumulative ductility and energy dissipation without undergoing any instability.

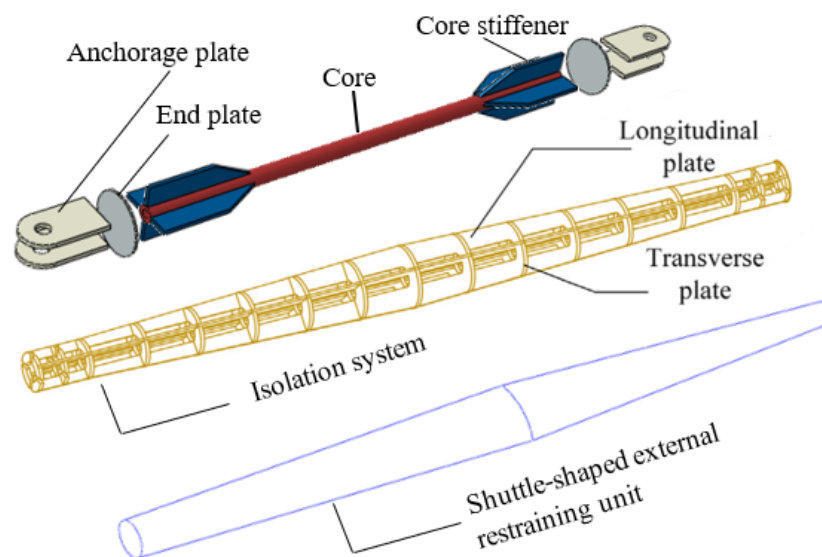


**Figure 19.** Configuration of Shuttle-shaped all-steel BRB [133].

### 3.4.3. Timber BRBs

In recent times, the use of timber as a structural material to construct multi-story buildings has swiftly magnified to assist in the reduction of carbon footprint for sustainability and environmental issues. Timber has also been used as a restraining component material of BRBs in the place of concrete/mortar and steel. Luo et al. [134] introduced a novel hybrid steel-timber BRB comprising a cross-shaped steel core component and timber restraining unit to enhance the seismic performance of timber-framed structures as shown in Figure 20. Eight specimens having 3600 mm in length were fabricated to examine the effects of different configurations and design parameters on the hysteretic behavior of newly proposed braces. Experiments were conducted on an especially established test setup and the fatigue-based axial cyclic load was applied through a hydraulic ram having 2000-kN load capacity. To measure the deformation of tested braces, five linear voltage displacement transducers (LVDT) were placed at different locations. The axial force-deformation curves of tested timber BRBs demonstrated that all braces provided stable hysteretic response throughout the loading protocol except T-BRB8, whose restraining unit ruptured prematurely and split at the ends.

Recently, Takeuchi et al. [135] has developed mass timber BRBs and conducted a comprehensive experimental study to investigate the bulging of weak and strong axes and failure modes of global buckling. In the first phase of the investigation, sub-assembly tests were performed on short and long specimens with varying features of core and restraining components to obtain distinctive bulging and global buckling capacities of the restrainers. Three long and seven small-length specimens, inclined at angles of 25 and 39 degrees, respectively, were tested on a sliding table. Based on the results of this section, four full-scale mass timber BRBs same as field size were designed and tested to validate the behavior of previously investigated braces. All full-scale specimens demonstrated stable hysteretic response and were able to achieve the expected tensile fracture failure mode of core components under low-cycle fatigue loadings. The study concluded that the mass timber BRBs justified the performance requirements of traditional BRBs specified in Japan and can be installed in structures as earthquake-resisting structural members. The authors also recommended the application of additional hardwood or steel reinforcing plates to reduce the chances of bulging failures and ensure reliable and stable hysteretic performance.

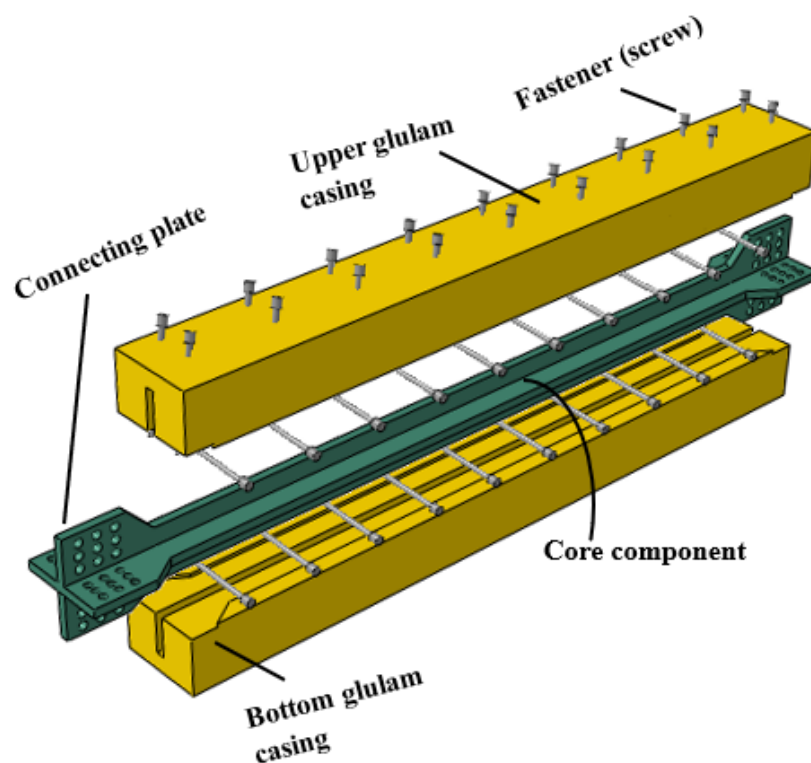


Figure 20. Composition of timber BRB [134].

### 3.5. Self-Centering BRBs

Residual deformations may arise in a structure when the metallic core component of BRB yields. However, these residual deformations can be minimized by employing a Self-Centering BRB. The SC-BRB combines an energy dissipation system with a self-centering mechanism. Essentially, an SC-BRB incorporates a conventional BRB along with a tensing element, such as a pre-tensioned rod or cable made from a unique material. This additional element generates a self-centering force, which effectively reduces inelastic or residual deformations in the structure. The concept of self-centering BRBs, which possess both energy dissipation capabilities and the ability to restore their original position following ground shaking, is relatively new and there have been only a few studies conducted on this innovative design.

In 2012, Miller et al. [136] developed a self-centering BRB which consisted of a typical concrete-filled BRB and super elastic nickel–titanium (NiTi) shape memory alloy (SMA) rods to provide additional energy dissipation and self-centering. As shown in Figure 21, the assembly of the proposed SC-BRB contained a steel plate core component which was tapered in the central region to make it appropriate for yielding. Three steel tubes were employed for different purposes as inner, middle, and outer tubes. Pea-gravel-based concrete was placed between the core and inner tube to prevent the buckling of the core component. The middle and outer tubes were welded to the left and right ends, respectively, and worked as a part of the load transfer system to carry compression forces. The pre-tensioned rods were connected to the brace portion using two anchorage end plates that govern the rods to stretch when the brace is in both compression and tension. Five large-scale specimens were designed, manufactured, and tested under cyclic loading and the results demonstrated that the proposed SMA SC-BRBs showed stable hysteretic behavior with significant self-centering ability and energy dissipation capacity.

Pre-stressed steel strands are the most widely used and cost-effective method for applying pre-stressed forces. To enhance the energy dissipation capabilities during earthquakes, Wang et al. [137] developed a self-centering BRB using cross-anchored pre-stressed steel strands. The proposed SC-BRB consisted primarily of two steel plate cores, three

steel tubes, and two sets of pre-stressed steel strands. The outer and middle tubes in the SC-BRB served two purposes. Firstly, they prevented the core plates from buckling when subjected to compression, thus contributing to the buckling restraint system. Secondly, these tubes could move relative to each other under tension and compression forces, resulting in the elongation of the pre-stressed steel strands. Once the external forces were released, the steel strands contracted, enabling self-centering behavior. The cross-anchored subsystem for self-centering was formed by the inner circular tube, two sets of parallel pre-stressed steel strands, and cover plates. This subsystem significantly increased the deformation capacity of the SC-BRB, nearly doubling it. The anchorage system used for the pre-stressed steel strands was of the clip type, a reliable and widely employed system in Chinese engineering practice.

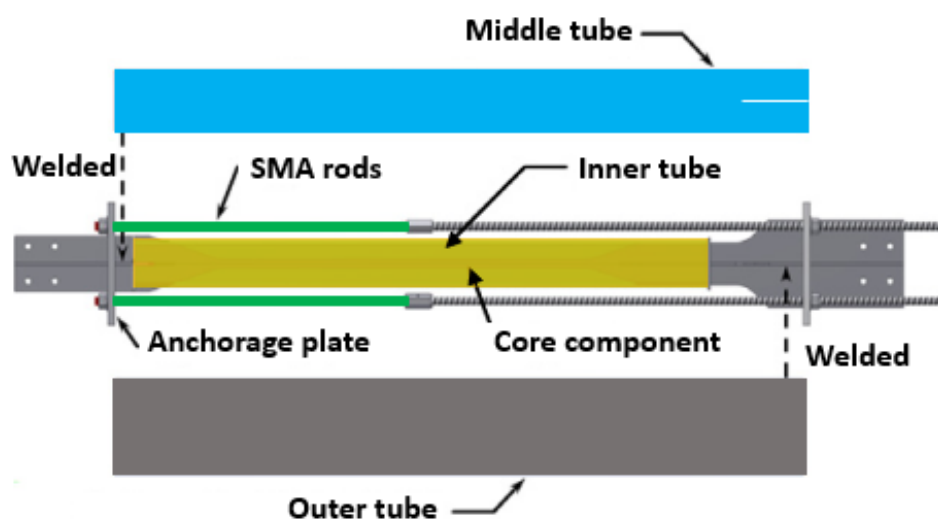


**Figure 21.** Composition of Self-Centering BRB [136].

It ensured that as the prestressing force increased, the gripping force also increased, preventing slippage between the steel strands and the anchor clips. To evaluate the energy dissipation and self-centering abilities of the proposed SC-BRB, two specimens utilizing cross-anchored pre-stressed strands were fabricated and tested. The SC-BRBs with appropriate parameters demonstrated favorable energy dissipation and self-centering capacity, maintaining effectiveness up to a deformation equal to 1% of the brace length.

To eliminate the residual drift of braced structures after a major lateral movement, Zhang [138] proposed an assembled self-centering BRB. The developed device was comprised of two systems: an energy dissipation and a self-centering system. The ED section was created to benefit from the core plate's stable metal yielding, which eliminates the need for concrete for buckling restraint. The key components of the self-centering arrangement were the outer and inner elements, along with pre-stressed disk springs containing link stoppers. The brace incorporated a feature that allowed for the partial substitution of fractured core and guiding plates by removing the clamping bolts in the steel channels and the high-strength bolts at the steel angles. Cyclic quasi-static experiments on four samples were conducted with various energy-dissipation ratios to summarize and empirically establish the hysteretic mechanics of the self-centering system. The seismic performance of frames proved that the newly developed braces were able to reduce the residual drifts substantially as compared to conventional-BRB frames with identical design parameters.

In another study, Zhou [139] presented a novel concept of self-centering BRBs by employing pretensioned basalt fiber-reinforced polymer (BFRP) composite tendons as self-centering part with two tubes containing two parallel steel plate cores for energy dissipation mechanism. Initially, tensile cyclic experiments were performed on two groups of tendons to examine the elongation capacity and elastic modulus. Following the satisfactory results

of tensile tests of tendons, two specimens of dual-tube self-centering BRB were tested under quasi-static loading with different areas of core plates. Prior to the failure of the self-centering system, both test samples consistently displayed the anticipated flag-shaped hysteresis response, accompanied by a relatively minor residual deformation. The effectiveness of the self-centering system was verified by measuring the internal forces in the Basalt Fiber-Reinforced Polymer (BFRP) tendons and the gaps between the tubes and end plates. Both specimens satisfied the criteria for ultimate ductility and cumulative ductility in braces.

Most recently, in 2023, Chen et al. [140] proposed an all-steel self-centering BRB by joining a simple-steel BRB and friction spring to overcome the deficiencies of steel strands and prestressed tendons. The proposed friction spring (SC-BRB) is constituted of two parts: an energy dissipation mechanism and a self-centering system, which are combined in series as shown in Figure 22. The BRB member includes an inner core component, debonding layers, exterior restraint plates, and end plates. The yielding region of the core component contains elliptical holes to concentrate plastic deformation in the perforated region and impedes premature failure of connection segments. Two different restraining plates have been used to impede the buckling of core components and provide space to install the friction spring for combining it with BRB. The SCS (Self-Centering System) comprises various components such as a friction spring, baffle plates, link stoppers, and rubber blocks. The friction spring is made up of inner and outer rings, with multiple pairs of these rings located between the left and right link stoppers. The baffle plates are firmly fastened to both sides of the friction spring and link stoppers. During cyclic loading, the baffle plates can move smoothly sideways the axial path of the brace, compressing the friction spring. To prevent deflection and dislocation of the rings, rubber blocks of four-quarter cylindrical shape are adhered to the stiffening rib, plugging the interior bay of the friction spring. The elastic rubber blocks allow for radial contraction of the friction spring under compression. Finally, after welding the blanking plate, the friction springs are pre-loaded using specialized equipment and adjusted using positioning bolts. The hysteretic response of the proposed SC-BRB was explored by performing two low-cycle fatigue experiments and the results show that the hysteresis curves of both specimens exhibited symmetric flag shapes. The authors advised that in order to achieve complete self-reset, the friction spring's minimum pre-pressure should be at least four times the yield force of the BRB.

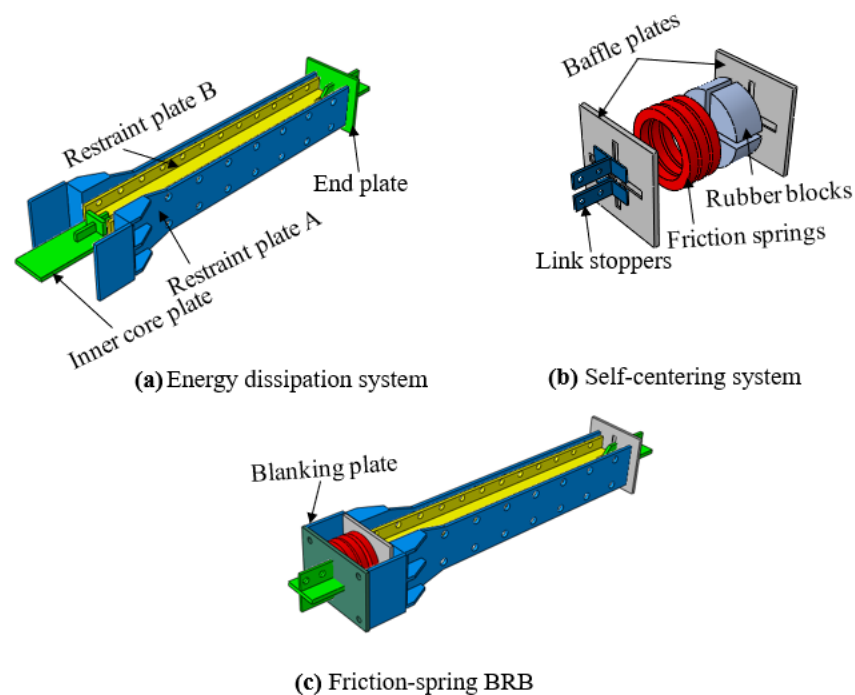


Figure 22. Composition of Friction-spring Self-centering BRB [140].

#### 4. Corrosion-Resistant BRBs

The exterior steel component of BRBs is susceptible to corrosion due to their installation in offshore structures and exposure to corrosive environments in factories. Aluminum, on the other hand, exhibits higher corrosion resistance and requires less maintenance, making it an excellent choice for construction in harsh locations. Xiang [141] developed a straightforward method for calibrating the plasticity parameter values of aluminum using coupon tests and created FE models of aluminum-BRBs. The analyzed BRB consisted of an outer circular tube and a core bar with a bamboo-like shape, where the parts with larger cross-sections resembled bamboo slubs. A stopper was incorporated in the middle of the BRB length to prevent rigid sliding between the core and the external units. Two specimens with varying lengths of plastic straining sections were designed using structural aluminum 6061-T6. The validation results demonstrated the effectiveness of the proposed method in capturing the cyclic plastic behavior of aluminum-BRBs. The authors also recommended conducting additional experimental tests to further investigate the application of this approach.

Deng et al. [142] introduced a lightweight and innovative Glass Fiber-Reinforced Polymer (GFRP) steel BRB as a substitute for heavy concrete-filled braces, making it suitable for challenging environments. The proposed BRB consisted of a steel core component and a restraining mechanism formed by four GFRP pultruded tubes securely bonded together with GFRP wrapping layers. They designed and tested six specimens, which were classified into two groups based on the wrapping methods, under quasi-static cyclic loading. The experiments focused on evaluating the energy dissipation capacities and ultimate failure patterns of the developed GFRP-Steel-BRBs. The results demonstrated satisfactory performance, and additional reinforcements were recommended to prevent local buckling of the cores and tubes at the ends. In another study, Dusicka et al. [143] presented an ultra-lightweight BRB by utilizing an aluminum-core component consisting of four equal-legged angles, which were restrained by bundled GFRP pultruded tubes. Detailed finite-element models of the proposed braces were developed, employing a constitutive model for the 6061-T6511 aluminum alloy. The study concluded that the ultra-lightweight BRB prototype met the requirements for global restraint and weighed only 27% and 41% of the conventional concrete-filled and all-steel BRB configurations, respectively.

Sun et al. [144] introduced a novel concrete-filled buckling-restrained brace BRB with a circular-shaped tube made of glass-fiber reinforced polymer (GFRP) as the exterior restraining member, as displayed in Figure 23. The replacement of the traditional steel exterior unit with GFRP tubes resulted in a 5–10% reduction in the self-weight of BRBs and offered a solution to mitigate corrosion-related issues. The experimental setup consisted of fourteen specimens, including 11 BRBs with GFRP tube braces and three with conventional steel sections, aiming to investigate the effects of constraint ratios and GFRP characteristics on the hysteretic performance of BRBs. Two types of GFRP elements, namely winding-pultrusion and filament winding tubes, fabricated using different processes and varying thicknesses, were utilized. Additionally, three types of material tests were conducted to evaluate the hoop tensile, longitudinal compressive, and tensile mechanical properties of GFRP samples. The findings revealed that GFRP exhibits an orthotropic nature compared to steel, with lower strength in the longitudinal direction but higher strength in the hoop direction. The study concluded that the GFRP tubes were effective in limiting local buckling of BRBs due to their higher hoop strengths, thus contributing less to preventing global buckling.

The wrapping of BRBs with fiber sheets can be a useful approach for corrosive environments. Jia et al. [145] proposed a novel concrete-filled assembled BRB, which consists of a steel plate core component and two steel channels filled with concrete, wrapped using basalt and carbon cloth to function as a restraining unit. The characteristics of basalt and carbon fibers were obtained from tensile tests, and eight specimens of assembled BRBs were assessed to examine their mechanical properties, hysteretic performance, and energy dissipation capacities under distinctive loading patterns. The experimental results demonstrated that the assembled BRBs were capable of providing adequate ductility and energy

dissipation capacities, and the fiber cloth did not show any rupture. Moreover, none of the specimens underwent global buckling, and their load-carrying capacities were lost due to the fracture of core components. The authors were satisfied with the performance requirements of the novel BRBs and recommended them as a beneficial alternative to conventional BRBs for use in hostile areas.

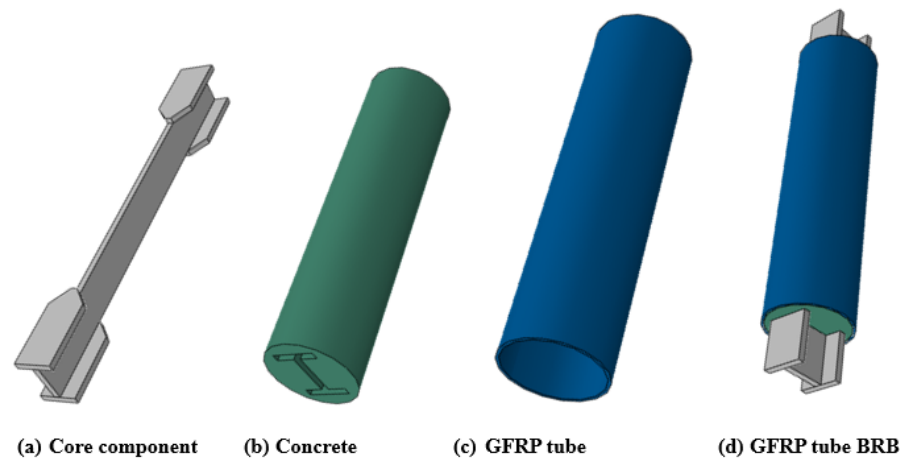


**Figure 23.** Fabrication of GFRP-BRBs [144].

Zhao et al. [146] developed a maintenance-free BRB by utilizing a rectangular tube made of glass fiber-reinforced polymer as the exterior restraining unit. As depicted in Figure 24, the core component consisted of a steel plate that was enclosed within the exterior tube, and the braces were manufactured using a vacuum-infused casting process to assemble all the components simultaneously. The restraining system incorporated GFRP ribs, which were formed by applying resin onto strips of polyurethane foam, encased with fiberglass cloth. Four specimens were evaluated to investigate their hysteretic responses, deformation capacities, and failure modes. The proposed maintenance-free braces demonstrated a lighter weight compared to traditional BRBs, and the results indicated that the tested specimens exhibited improved performance under small displacement loading cycles and maintained good structural integrity.

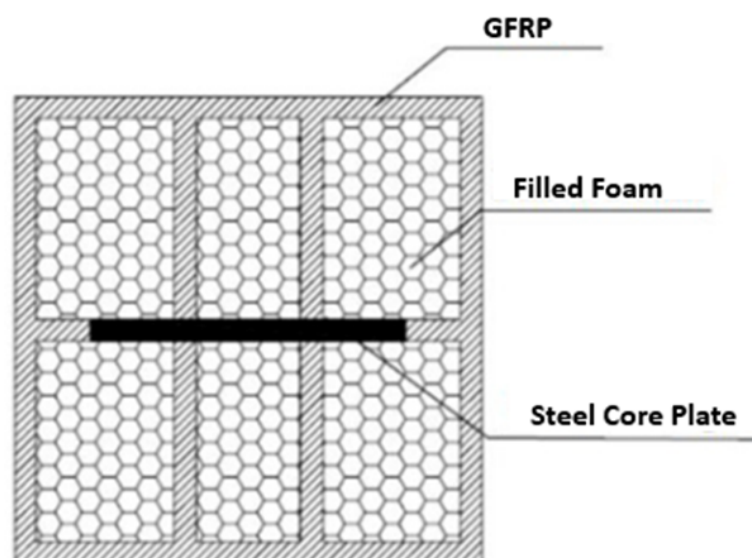


**Figure 24.** Configuration of Maintenance-free BRB [146].

Buckling-restrained brace BRB frames employ strength-adjustment factors in the design of different elements. The compressive strength adjustment factor, denoted as ( $\beta$ ), represents the ratio of the maximum compressive force to the maximum tensile force observed during the testing of BRB specimens. This factor characterizes the amplification of compressive strength, resulting from the combined effects of Poisson's ratio and the frictional resistance between the core component and restraining unit of BRBs under compression loading. In Figure 25, a comparison of compressive strength-adjustment factors for various BRBs is presented and notably, the majority of these values remain within the specified limit of ( $\beta = 1.3$ ), as outlined in the code ANSI/AISC 341-10 [147]. This limit serves as a critical criterion to ensure the structural integrity and safety of the BRB frames.

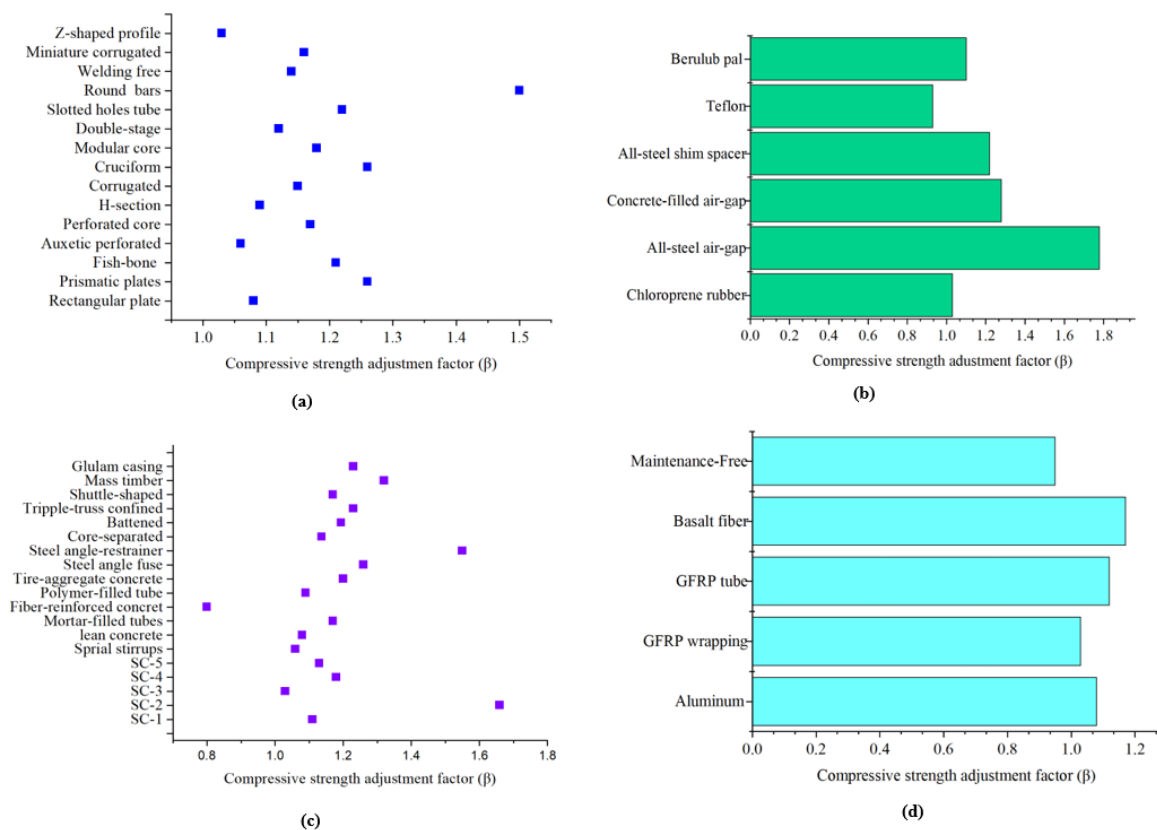


**Figure 25.** Comparison of compressive strength adjustment factors ( $\beta$ ) for different types of BRBs based on (a) Core shapes (b) Unbonding materials (c) Restraining units and self-centering (d) Corrosion resistant.

As shown in Figure 25a, distinctive core shapes were introduced for the development of novel buckling-restrained braces (BRBs) to enhance their performance. For the majority of these BRB types, the hysteretic response remained stable with the  $\beta$  values in the range of 1.0–1.3. However, the value of  $\beta$  reached 1.5 for round-bars BRBs, indicating a slightly different behavior compared to other BRB types. In the case of comparison for unbonding materials shown in Figure 25b, the maximum value of  $\beta$  as 1.78 was observed in the evaluation of all-steel BRB with only air-gap. The absence of unbonding materials created jamming and gradually increased the friction forces between the core and restraining components, which ultimately led to a substantially higher compression strength adjustment factor, and it was recommended to install unbonding layers to achieve better performance of all-steel BRBs. Restraining components have an imperative role in the performance of BRBs because the maximum compressive and tensile strength of BRBs depend on the stiffening capacity of these elements to prevent the core from buckling and ensure a symmetrical hysteretic response. Figure 25c demonstrates that most of the

recently proposed restraining materials acquired satisfactory results except steel angle-restrainer and self-centering BRBs with cross-anchored strands which showed higher  $\beta$  of 1.55 and 1.67, respectively. The response of corrosion-resistant BRBs, which focused on the concerns related to corrosive and harsh environments, is shown in Figure 25d and it was found that all specimens exhibited adequate response with ( $\beta = 0.95$ – $1.17$ ) and symmetrical hysteresis characteristics.

## 5. Conclusions and Future Directions

This paper presents a comprehensive systematic literature review focusing on the development of distinct types of BRBs. With an intensive examination of articles published in top-quality journals between 2009 and 2023, this study categorizes the developed BRBs based on their constitutive components. The analysis reveals that most studies concentrated on creating distinct configurations of brace components using carbon steel. The performance evaluation of BRBs is primarily centered around their hysteretic response and energy dissipation capacities. The inelastic deformation capacity of the brace core under repeated cyclic loading and the stability of the outer restraining unit are the two key factors that determine the overall effectiveness of the BRBs. The exterior restraint system needs to be rigid and have satisfactory stiffness and strength to stop the core component from buckling globally while still allowing the yielding core zone to buckle in a higher mode. Inadequate thickness of the restraining elements can lead to local buckling failure, which, in turn, can induce additional eccentricity in the deformed core component and result in overall flexural buckling of the BRBs. As shown in Figure 26, the majority of earlier studies were conducted by employing carbon steel for the restraining units. When BRB frames are used in humid and coastal locations, the exterior steel restraining element can become susceptible because steel corrodes with time and loses mass while also degrading its mechanical properties. Therefore, the detrimental impact of corrosion on BRBs in corrosive and coastal environments cannot be overlooked. To withstand strong earthquakes, it becomes essential to study the influence of corrosion on the seismic behavior and energy dissipation capacities of BRBs. This comprehensive review highlights the limited research on braces employing anti-corrosive materials, with only a few studies exploring the use of fiber-reinforced polymers and aluminum alloys. It suggests numerous prospective areas for future research to enhance the performance of BRBs.

Future improvements in the performance of BRBs necessitate exploring the impact of corrosion on their hysteretic properties. There is a need to conduct component and subassembly level investigations to evaluate the effects of corrosion on ductility, energy dissipation capacity, and failure mode of BRBs. In terms of alternative materials, aluminum alloy presents favorable characteristics such as lightweight, high strength-to-weight ratio, corrosion resistance, durability, and recyclability. However, there have been only five studies on BRBs fabricated with aluminum alloy, necessitating further investigation, especially under simulated corrosive conditions.

Similarly, stainless steel offers exceptional durability, ductility, and corrosion resistance. While some studies have used stainless-steel plates and bars for hybrid core components in BRBs, no research has focused on fabricating the entire BRB using stainless steel and analyzing its behavior. Consequently, there is a crucial need for experimental research to explore the seismic performance of BRBs entirely made of stainless steel.

It is necessary to conduct structural-level studies that incorporate new materials and consider corrosive features to advance the code provisions and design guidelines that were originally developed based on the behavior of conventional BRB frames. These studies will contribute to the advancement of BRB technology and ensure that the code provisions and design guidelines are updated to reflect the behavior and performance of BRBs utilizing innovative materials and accounting for corrosive environments.

By addressing these research gaps, the field of BRBs can advance and contribute to the development of more resilient and corrosion-resistant seismic-resistant structures.

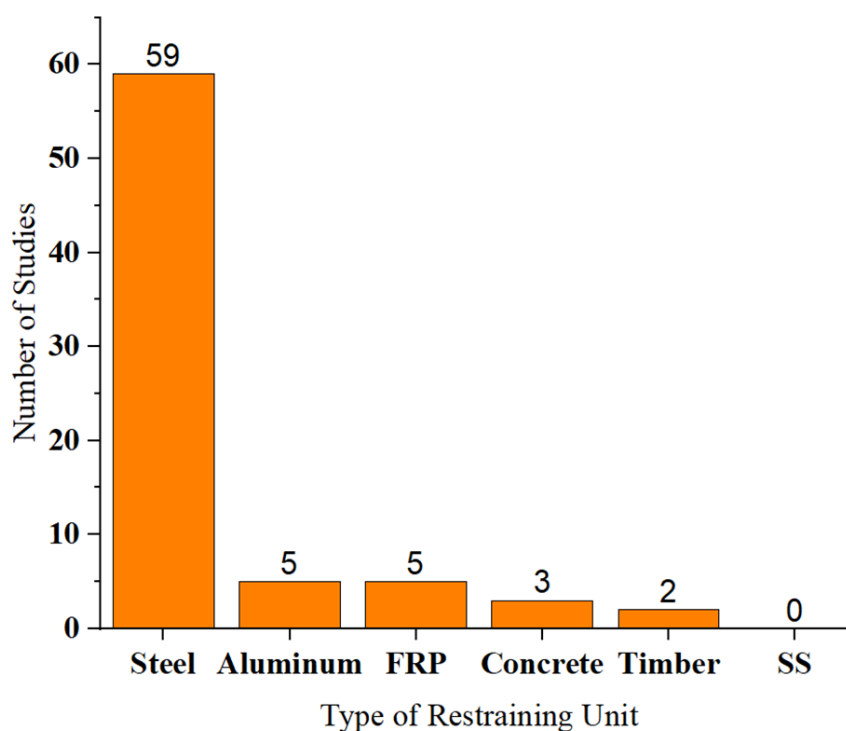


**Figure 26.** Distribution of Studies by Restraining Units.

**Author Contributions:** Conceptualization, H.H. and D.-K.K.; methodology, H.H. and D.-K.K.; software, H.H. and D.-K.K.; validation, H.H. and D.-K.K.; formal analysis, H.H. and D.-K.K.; resources, H.H. and D.-K.K.; writing—original draft preparation, H.H. and D.-K.K.; writing—review and editing, H.H. and D.-K.K.; visualization, H.H. and D.-K.K.; supervision, D.-K.K.; funding acquisition, D.-K.K. All authors have read and agreed to the published version of the manuscript.

**Funding:** This work was supported by the Basic Science Research Program through the National Research Foundation (NRF) funded by the Korea Ministry of Education (No. 2022R1F1A1076048).

**Data Availability Statement:** Data available within the article.

**Conflicts of Interest:** The authors declare no conflict of interest.

## References

- Pavel, F. Seismic Design Codes—Key Elements for Seismic Risk Perception and Reduction in Europe. *Buildings* **2023**, *13*, 158. [CrossRef]
- Mavrouli, M.; Mavroulis, S.; Lekkas, E.; Tsakris, A. An emerging health crisis in Turkey and Syria after the earthquake disaster on 6 february 2023: Risk factors, prevention and management of infectious diseases. *Healthcare* **2023**, *11*, 1022. [CrossRef]
- AIR Worldwide. Study of Impact and the Insurance and Economic Cost of a Major Earthquake in British Columbia and Ontario/Québec. 2013. Available online: <http://assets.ibc.ca/Documents/Studies/IBC-EQ-Study-Summary.pdf> (accessed on 1 June 2023).
- Sharafi, P.; Mortazavi, M.; Usefi, N.; Kildashti, K.; Ronagh, H.; Samali, B. Lateral force resisting systems in lightweight steel frames: Recent research advances. *Thin-Walled Struct.* **2018**, *130*, 231–253. [CrossRef]
- Saaed, T.E.; Nikolakopoulos, G.; Jonasson, J.E.; Hedlund, H. A state-of-the-art review of structural control systems. *J. Vib. Control* **2015**, *21*, 919–937. [CrossRef]
- Ghaedi, K.; Ibrahim, Z.; Adeli, H.; Javanmardi, A. Invited Review: Recent developments in vibration control of building and bridge structures. *J. Vibroeng.* **2017**, *19*, 3564–3580. [CrossRef]
- Titirla, M.; Katakalos, K.; Zuccaro, G.; Fabbrocino, F. On the mechanical modeling of an innovative energy dissipation device. *Ing. Sismica Int. J. Earthq. Eng.* **2017**, *34*, 126–138.
- Titirla, M.D.; Papadopoulos, P.K.; Doudoumis, I.N. Finite element modelling of an innovative passive energy dissipation device for seismic hazard mitigation. *Eng. Struct.* **2018**, *168*, 218–228. [CrossRef]
- Titirla, M.; Katakalos, K. Evaluation of an innovative passive mitigation device through experimental and numerical investigation. In Proceedings of the 6th International Conference on Computational Methods in Structural Dynamics and Earthquake Engineering, Rhodes Island, Greece, 15–17 June 2017.

10. Kim, J.; Kim, M.C.; Kim, D.K. Preliminary study on a composite steel slit damper. *J. Mech. Sci. Technol.* **2021**, *35*, 3931–3942. [[CrossRef](#)]
11. Titirla, M.; Papadopoulos, P.K.; Doudoumis, I.N.; Katakalos, K. Cyclic response of an antisismic steel device for building—An experimental and numerical study. In Proceedings of the 16TH World Conference on Earthquake Engineering, Santiago, Chile, 9–13 January 2017; pp. 9–13.
12. Özkılıç, Y.O.; Bozkurt, M.B. Numerical validation on novel replaceable reduced beam section connections for moment-resisting frames. In *Structures*; Elsevier: Amsterdam, The Netherlands, 2023, Volume 50, pp. 63–79. [[CrossRef](#)]
13. Özkılıç, Y.O. Cyclic and monotonic performance of stiffened extended end-plate connections with large-sized bolts and thin end-plates. *Bull. Earthq. Eng.* **2022**, *20*, 7441–7475. [[CrossRef](#)]
14. Özkılıç, Y.O. A new replaceable fuse for moment resisting frames: Replaceable bolted reduced beam section connections. *Steel Compos. Struct.* **2020**, *35*, 353–370.
15. Özkılıç, Y.O. Cyclic and monotonic performance of unstiffened extended end-plate connections having thin end-plates and large-bolts. *Eng. Struct.* **2023**, *281*, 115794. [[CrossRef](#)]
16. Azad, S.K.; Topkaya, C. A review of research on steel eccentrically braced frames. *J. Constr. Steel Res.* **2017**, *128*, 53–73. [[CrossRef](#)]
17. Annan, C.; Youssef, M.; El Naggar, M. Experimental evaluation of the seismic performance of modular steel-braced frames. *Eng. Struct.* **2009**, *31*, 1435–1446. [[CrossRef](#)]
18. Qu, Z.; Kishiki, S.; Maida, Y.; Sakata, H.; Wada, A. Seismic responses of reinforced concrete frames with buckling restrained braces in zigzag configuration. *Eng. Struct.* **2015**, *105*, 12–21. [[CrossRef](#)]
19. Abbaszadeh, A.; Chaallal, O. Enhancing resilience and self-centering of existing RC coupled and single shear walls using EB-FRP: State-of-the-art review and research needs. *J. Compos. Sci.* **2022**, *6*, 301. [[CrossRef](#)]
20. Singhal, S.; Chourasia, A.; Chellappa, S.; Parashar, J. Precast reinforced concrete shear walls: State of the art review. *Struct. Concr.* **2019**, *20*, 886–898. [[CrossRef](#)]
21. Javanmardi, A.; Ibrahim, Z.; Ghaedi, K.; Benisi Ghadim, H.; Hanif, M.U. State-of-the-art review of metallic dampers: testing, development and implementation. *Arch. Comput. Methods Eng.* **2020**, *27*, 455–478. [[CrossRef](#)]
22. Özkılıç, Y.O.; Topkaya, C. Extended end-plate connections for replaceable shear links. *Eng. Struct.* **2021**, *240*, 112385. [[CrossRef](#)]
23. Özkılıç, Y.O.; Bozkurt, M.B.; Topkaya, C. Mid-spliced end-plated replaceable links for eccentrically braced frames. *Eng. Struct.* **2021**, *237*, 112225. [[CrossRef](#)]
24. Özkılıç, Y.O. Optimized stiffener detailing for shear links in eccentrically braced frames. *Steel Compos. Struct. Int. J.* **2021**, *39*, 35–50.
25. Özkılıç, Y.O. Interaction of flange and web slenderness, overstrength factor and proposed stiffener arrangements for long links. *J. Constr. Steel Res.* **2022**, *190*, 107150. [[CrossRef](#)]
26. Özkılıç, Y.O.; Zeybek, Ö.; Topkaya, C. Stability of laterally unsupported shear links in eccentrically braced frames. *Earthq. Eng. Struct. Dyn.* **2022**, *51*, 832–852. [[CrossRef](#)]
27. Hussain, H.; Gao, X.; Shi, A. A Finite Element Study on Compressive Resistance Degradation of Square and Circular Steel Braces under Axial Cyclic Loading. *Appl. Sci.* **2021**, *11*, 6094. [[CrossRef](#)]
28. Titirla, M.D. A State-of-the-Art Review of Passive Energy Dissipation Systems in Steel Braces. *Buildings* **2023**, *13*, 851. [[CrossRef](#)]
29. Clark, P. Design procedures for buildings incorporating hysteretic damping devices. In Proceedings of the International Post-SMiRT Conference Seminar on Seismic Isolation, Cheju, Republic of Korea, 23–25 August 1999.
30. Black, C.J.; Makris, N.; Aiken, I.D. Component testing, seismic evaluation and characterization of buckling-restrained braces. *J. Struct. Eng.* **2004**, *130*, 880–894. [[CrossRef](#)]
31. Bozkurt, M.B.; Özkılıç, Y.O.; Topkaya, C. Determination of Displacement Amplification Factors for Chevron BRBFs. 2017. Available online: [http://eeme.ntua.gr/proceedings/9th/Papers/055\\_PAP\\_Bozkurt.pdf](http://eeme.ntua.gr/proceedings/9th/Papers/055_PAP_Bozkurt.pdf) (accessed on 1 June 2023).
32. Yoshino, T.; Karino, Y. Experimental study on shear wall with braces: Part 2. In *Summaries of Technical Papers of Annual Meeting*; Architectural Institute of Japan, Structural Engineering Section: Tokyo, Japan, 1971; Volume 11, pp. 403–404.
33. Xie, Q. State of the art of buckling-restrained braces in Asia. *J. Constr. Steel Res.* **2005**, *61*, 727–748. [[CrossRef](#)]
34. Kimura, K.; Yoshioka, K.; Takeda, T.; Fukuya, Z.; Takemoto, K. Tests on braces encased by mortar in-filled steel tubes. In *Summaries of Technical Papers of Annual Meeting*; Architectural Institute of Japan: Tokyo, Japan, 1976; Volume 1041, pp. 1–42.
35. Takahashi, S.; Mochizuki, N. Experimental study on buckling of unbonded braces under axial compressive force: Part 1. In *Proceedings of the Summaries of Technical Papers of Annual Meeting*; Architectural Institute of Japan: Tokyo, Japan, 1979; pp. 1623–1626.
36. Mochizuki, S.; Murata, Y.; Andou, N.; Takahashi, S. Experimental study on buckling of unbonded braces under axial forces: Part 4. In *Summaries of Technical Papers of Annual Meeting*; Architectural Institute of Japan: Tokyo, Japan, 1982; pp. 2263–2264.
37. Fujimoto, M.; Wada, A.; Saeki, E. A study on the unbonded brace encasted in buckling-restrained concrete and steel tube. *J. Str. Eng. AIJ* **1988**, *34*, 249–258.
38. Miller, D.K. Lessons learned from the Northridge earthquake. *Eng. Struct.* **1998**, *20*, 249–260. [[CrossRef](#)]
39. Sabol, T.A. An assessment of seismic design practice of steel structures in the United States since the Northridge earthquake. *Struct. Des. Tall Spec. Build.* **2004**, *13*, 409–423. [[CrossRef](#)]

40. Tremblay, R.; Bolduc, P.; Neville, R.; DeVall, R. Seismic testing and performance of buckling-restrained bracing systems. *Can. J. Civ. Eng.* **2006**, *33*, 183–198. [CrossRef]
41. Zhou, Y.; Shao, H.; Cao, Y.; Lui, E.M. Application of buckling-restrained braces to earthquake-resistant design of buildings: A review. *Eng. Struct.* **2021**, *246*, 112991. [CrossRef]
42. Bozkurt, M.B.; Ozkılıç, Y.O.; Topkaya, C. Evaluation of Displacement Amplification Factors for Steel Buckling Restrained Braced Frames. 2016. Available online: <https://hdl.handle.net/11511/55411> (accessed on 1 June 2023).
43. Bozkurt, M.B.; Özkılıç, Y.O.; Topkaya, C. Evaluation of Seismic Performance Factors for Chevron Buckling Restrained Braced Frames. 2017. Available online: <https://hdl.handle.net/11511/80526> (accessed on 1 June 2023).
44. Eryaşar, M.E.; Topkaya, C. An experimental study on steel-encased buckling-restrained brace hysteretic dampers. *Earthq. Eng. Struct. Dyn.* **2010**, *39*, 561–581. [CrossRef]
45. D’Aniello, M.; Della Corte, G.; Landolfo, R. Finite element modelling and analysis of “all-steel” dismountable buckling restrained braces. *Open Constr. Build. Technol. J.* **2014**, *8*, 216–226. [CrossRef]
46. Qu, B.; Liu, X.; Hou, H.; Qiu, C.; Hu, D. Testing of buckling-restrained braces with replaceable steel angle fuses. *J. Struct. Eng.* **2018**, *144*, 04018001. [CrossRef]
47. Özkılıç, Y.O.; Bozkurt, M.B.; Topkaya, C. Evaluation of seismic response factors for BRBFs using FEMA P695 methodology. *J. Constr. Steel Res.* **2018**, *151*, 41–57. [CrossRef]
48. ÖZKILIÇ, Y.O. The Effects of Steel Core Imperfection, Gap Size and Friction Coefficient on the Behavior of All-Steel Buckling Restrained Braces. *DÜZCE ÜNİV. BİLİM TEKNOL. DERG.* **2021**, *9*, 1342–1357. [CrossRef]
49. Zhuge, Y.; Ma, X.; Zeng, J. Recent progress in buckling restrained braces: A review on material development and selection. *Adv. Struct. Eng.* **2022**, *25*, 1549–1564. [CrossRef]
50. ÖZKILIÇ, Y.O. Evaluation of Seismic Performance Factors for Buckling Restrained Braced Frames. Ph.D Thesis, Middle East Technical University, Ankara, Turkey, 2016.
51. Luo, L.; Fu, H.; Zhang, Y.; Xie, X. Experimental study on the overall stability of corroded H-Shaped steel beams. *Buildings* **2022**, *12*, 1923. [CrossRef]
52. Ahn, J.H.; Jeon, S.H.; Jeong, Y.S.; Cho, K.I.; Huh, J. Evaluation of residual compressive strength and behavior of corrosion-damaged carbon steel tubular members. *Materials* **2018**, *11*, 1254. [CrossRef]
53. Xu, S.; Zhang, Z.; Qin, G. Study on the seismic performance of corroded H-shaped steel columns. *Eng. Struct.* **2019**, *191*, 39–61. [CrossRef]
54. Zhang, Z.; Xu, S.; Wang, H.; Nie, B.; Su, C. Flexural buckling behavior of corroded hot-rolled H-section steel beams. *Eng. Struct.* **2021**, *229*, 111614. [CrossRef]
55. Wang, H.; Xu, S.; Li, A.; Kang, K. Experimental and numerical investigation on seismic performance of corroded welded steel connections. *Eng. Struct.* **2018**, *174*, 10–25. [CrossRef]
56. Zhang, Z.; Xu, S.; Li, R. Comparative investigation of the effect of corrosion on the mechanical properties of different parts of thin-walled steel. *Thin-Walled Struct.* **2020**, *146*, 106450. [CrossRef]
57. Zhao, X.L.; Zhang, L. State-of-the-art review on FRP strengthened steel structures. *Eng. Struct.* **2007**, *29*, 1808–1823. [CrossRef]
58. Ye, Y.Y.; Zeng, J.J.; Li, P.L. A State-of-the-Art Review of FRP-Confined Steel-Reinforced Concrete (FCSRC) Structural Members. *Polymers* **2022**, *14*, 677. [CrossRef]
59. Shedge, H.; Patil, N.; Tapase, A.; Kadam, D.; Shelar, A.; Bobade, S. A State of the Art Review of Buckling Restrained Brace: History, Application, and Design. In *Advanced Geotechnical and Structural Engineering in the Design and Performance of Sustainable Civil Infrastructures: Proceedings of the 6th GeoChina International Conference on Civil & Transportation Infrastructures: From Engineering to Smart & Green Life Cycle Solutions—Nanchang, China, 19–21 July 2021*; Springer: Cham, Switzerland, 2021; pp. 43–52. [CrossRef]
60. Tupenaite, L.; Kanapeckiene, L.; Naimaviciene, J.; Kaklauskas, A.; Gecys, T. Timber Construction as a Solution to Climate Change: A Systematic Literature Review. *Buildings* **2023**, *13*, 976. [CrossRef]
61. Payawal, J.M.G.; Kim, D.K. Image-Based Structural Health Monitoring: A Systematic Review. *Appl. Sci.* **2023**, *13*, 968. [CrossRef]
62. Gregory, A.T.; Denniss, A.R. An introduction to writing narrative and systematic reviews—Tasks, tips and traps for aspiring authors. *Hear. Lung Circ.* **2018**, *27*, 893–898. [CrossRef]
63. Bozkurt, M.B.; Özkılıç, Y.O.; Topkaya, C. Effects of Different Core Plate Properties on Global Response of BRBFs. 2017. Available online: [http://eeme.ntua.gr/proceedings/9th/Papers/056\\_PAP\\_Bozkurt.pdf](http://eeme.ntua.gr/proceedings/9th/Papers/056_PAP_Bozkurt.pdf) (accessed on 1 June 2023).
64. ASTM A36/A36M-12; Standard specification for Carbon Structural Steel. ASTM: West Conshohocken, PA, USA, 2014.
65. JIS G3101; Rolled Steel for General Structure. Japanese Standards Association: Tokyo, Japan, 1987.
66. GB/T700-2006; General Administration of Quality Supervision, Inspection and Quarantine of The People’s Republic of China. Carbon Structural Steel. Standardization Administration of the People’s Republic of China (SAC): Beijing, China, 2006.
67. Usami, T.; Wang, C.L.; Funayama, J. Developing high-performance aluminum alloy buckling-restrained braces based on series of low-cycle fatigue tests. *Earthq. Eng. Struct. Dyn.* **2012**, *41*, 643–661. [CrossRef]
68. Shi, G.; Gao, Y.; Wang, X. Material properties and partial factors for resistance of low yield point steels in China. *Constr. Build. Mater.* **2019**, *209*, 295–305. [CrossRef]
69. Rossi, B. Discussion on the use of stainless steel in constructions in view of sustainability. *Thin-Walled Struct.* **2014**, *83*, 182–189. [CrossRef]

70. Gardner, L. Stability and design of stainless steel structures—Review and outlook. *Thin-Walled Struct.* **2019**, *141*, 208–216. [[CrossRef](#)]
71. Dabbagh, N.M.R.; Al Zand, A.W.; Liejy, M.C.; Ansari, M.; Tawfeeq, W.M.; Badaruzzaman, W.H.W.; Kaish, A.; Yaseen, Z.M. Strengthening Behavior of Rectangular Stainless Steel Tube Beams Filled with Recycled Concrete Using Flat CFRP Sheets. *Buildings* **2023**, *13*, 1102. [[CrossRef](#)]
72. Chacón, R.; Vega, A.; Mirambell, E. Numerical study on stainless steel I-shaped links on eccentrically braced frames. *J. Constr. Steel Res.* **2019**, *159*, 67–80. [[CrossRef](#)]
73. Al-Sadoon, Z.A.; Karzad, A.S.; Sagheer, A.; AlHamaydeh, M. Replaceable fuse buckling-restrained brace (BRB): Experimental cyclic qualification testing and NLFEA modeling. In *Structures*; Elsevier: Amsterdam, The Netherlands, 2022; Volume 39, pp. 997–1015. [[CrossRef](#)]
74. Ghowsi, A.F.; Sahoo, D.R.; Kumar, P.A. Cyclic tests on hybrid buckling-restrained braces with Fe-based SMA core elements. *J. Constr. Steel Res.* **2020**, *175*, 106323. [[CrossRef](#)]
75. Jiang, T.; Dai, J.; Yang, Y.; Liu, Y.; Bai, W. Study of a new-type of steel buckling-restrained brace. *Earthq. Eng. Eng. Vib.* **2020**, *19*, 239–256. [[CrossRef](#)]
76. Shi, Q.X.; Wang, F.; Wang, P.; Chen, K. Experimental and numerical study of the seismic performance of an all-steel assembled Q195 low-yield buckling-restrained brace. *Eng. Struct.* **2018**, *176*, 481–499. [[CrossRef](#)]
77. Huang, F.; Duan, H.; Cheng, B.; Teng, N. Hysteretic performance of all-steel assembled double-cores buckling-restrained braces using Q195 low-yield core. *J. Constr. Steel Res.* **2021**, *187*, 106925. [[CrossRef](#)]
78. Wang, J.; Shi, Y.; Wang, Y. Constitutive model of low-yield point steel and its application in numerical simulation of buckling-restrained braces. *J. Mater. Civ. Eng.* **2016**, *28*, 04015142. [[CrossRef](#)]
79. Qiu, C.; Zhang, A.; Jiang, T.; Du, X. Seismic performance analysis of multi-story steel frames equipped with FeSMA BRBs. *Soil Dyn. Earthq. Eng.* **2022**, *161*, 107392. [[CrossRef](#)]
80. Al-Sadoon, Z.A.; Saatcioglu, M.; Palermo, D. New buckling-restrained brace for seismically deficient reinforced concrete frames. *J. Struct. Eng.* **2020**, *146*, 04020082. [[CrossRef](#)]
81. Lanning, J.; Benzoni, G.; Uang, C.M. Using buckling-restrained braces on long-span bridges. I: Full-scale testing and design implications. *J. Bridge Eng.* **2016**, *21*, 04016001. [[CrossRef](#)]
82. Avci-Karatas, C.; Celik, O.C.; Yalcin, C. Experimental investigation of aluminum alloy and steel core buckling restrained braces (BRBs). *Int. J. Steel Struct.* **2018**, *18*, 650–673. [[CrossRef](#)]
83. Wang, C.L.; Usami, T.; Funayama, J.; Imase, F. Low-cycle fatigue testing of extruded aluminium alloy buckling-restrained braces. *Eng. Struct.* **2013**, *46*, 294–301. [[CrossRef](#)]
84. Proença, J.M.; Ferreira, R.; Gago, A.S. Seismic Retrofit of Pilotis Buildings by Novel Aluminium Buckling-Restrained Braces (Al-BRBs). Application to a Modernist Architecture Building in Lisbon. *Int. J. Archit. Herit.* **2023**, 1–22. [[CrossRef](#)]
85. Tabatabaei, S.A.R.; Mirghaderi, S.R.; Hosseini, A. Experimental and numerical developing of reduced length buckling-restrained braces. *Eng. Struct.* **2014**, *77*, 143–160. [[CrossRef](#)]
86. Xu, F.; Chen, J.; Shu, K.; Su, M.n. Cyclic behaviour of double-tube buckling-restrained braces for boiler steel plant structures. *J. Constr. Steel Res.* **2018**, *150*, 556–569. [[CrossRef](#)]
87. Hoveidae, N.; Radpour, S. A novel all-steel buckling restrained brace for seismic drift mitigation of steel frames. *Bull. Earthq. Eng.* **2021**, *19*, 1537–1567. [[CrossRef](#)]
88. Dehghani, M.; Tremblay, R. Design and full-scale experimental evaluation of a seismically enduring steel buckling-restrained brace system. *Earthq. Eng. Struct. Dyn.* **2018**, *47*, 105–129. [[CrossRef](#)]
89. Wang, C.L.; Usami, T.; Funayama, J. Improving low-cycle fatigue performance of high-performance buckling-restrained braces by toe-finished method. *J. Earthq. Eng.* **2012**, *16*, 1248–1268. [[CrossRef](#)]
90. Seker, O.; Shen, J. Developing an all-steel buckling controlled brace. *J. Constr. Steel Res.* **2017**, *131*, 94–109. [[CrossRef](#)]
91. Kim, D.H.; Lee, C.H.; Ju, Y.K.; Kim, S.D. Subassembly test of buckling-restrained braces with H-shaped steel core. *Struct. Des. Tall Spec. Build.* **2015**, *24*, 243–256. [[CrossRef](#)]
92. Atlayan, O.; Charney, F.A. Hybrid buckling-restrained braced frames. *J. Constr. Steel Res.* **2014**, *96*, 95–105. [[CrossRef](#)]
93. Wang, C.L.; Qing, Y.; Wang, J.; Chen, G.; Zeng, B. A new buckling-restrained brace with gap-supported tendon protection: Experiment and application. *Eng. Struct.* **2019**, *200*, 109688. [[CrossRef](#)]
94. Sitler, B.; Takeuchi, T.; Matsui, R.; Terashima, M.; Terazawa, Y. Experimental investigation of a multistage buckling-restrained brace. *Eng. Struct.* **2020**, *213*, 110482. [[CrossRef](#)]
95. Mirtaheri, M.; Gheidi, A.; Zandi, A.P.; Alanjari, P.; Samani, H.R. Experimental optimization studies on steel core lengths in buckling restrained braces. *J. Constr. Steel Res.* **2011**, *67*, 1244–1253. [[CrossRef](#)]
96. Xu, W.; Pantelides, C.P. Strong-axis and weak-axis buckling and local bulging of buckling-restrained braces with prismatic core plates. *Eng. Struct.* **2017**, *153*, 279–289. [[CrossRef](#)]
97. Jia, L.J.; Ge, H.; Maruyama, R.; Shinohara, K. Development of a novel high-performance all-steel fish-bone shaped buckling-restrained brace. *Eng. Struct.* **2017**, *138*, 105–119. [[CrossRef](#)]
98. Zhang, Y.; Ren, X.; Zhang, X.Y.; Huang, T.T.; Sun, L.; Xie, Y.M. A novel buckling-restrained brace with auxetic perforated core: Experimental and numerical studies. *Eng. Struct.* **2021**, *249*, 113223. [[CrossRef](#)]

99. Piedrafita, D.; Cahis, X.; Simon, E.; Comas, J. A new perforated core buckling restrained brace. *Eng. Struct.* **2015**, *85*, 118–126. [[CrossRef](#)]
100. Alemayehu, R.W.; Kim, Y.; Bae, J.; Ju, Y.K. Cyclic load test and finite element analysis of novel buckling-restrained brace. *Materials* **2020**, *13*, 5103. [[CrossRef](#)] [[PubMed](#)]
101. Ebadi Jamkhaneh, M.; Homaioon Ebrahimi, A.; Shokri Amiri, M. Investigation of the seismic behavior of brace frames with new corrugated all-steel buckling restrained brace. *Int. J. Steel Struct.* **2019**, *19*, 1225–1236. [[CrossRef](#)]
102. Zhao, J.; Wu, B.; Ou, J. A novel type of angle steel buckling-restrained brace: Cyclic behavior and failure mechanism. *Earthq. Eng. Struct. Dyn.* **2011**, *40*, 1083–1102. [[CrossRef](#)]
103. Piedrafita, D.; Cahis, X.; Simon, E.; Comas, J. A new modular buckling restrained brace for seismic resistant buildings. *Eng. Struct.* **2013**, *56*, 1967–1975. [[CrossRef](#)]
104. Sun, J.; Pan, P.; Wang, H. Development and experimental validation of an assembled steel double-stage yield buckling restrained brace. *J. Constr. Steel Res.* **2018**, *145*, 330–340. [[CrossRef](#)]
105. Dongbin, Z.; Xin, N.; Peng, P.; Mengzi, W.; Kailai, D.; Yabin, C. Experimental study and finite element analysis of a buckling-restrained brace consisting of three steel tubes with slotted holes in the middle tube. *J. Constr. Steel Res.* **2016**, *124*, 1–11. [[CrossRef](#)]
106. Zhang, S.; Tagawa, H.; Chen, X. Study on buckling-restrained braces using multiple round steel core bars. *J. Constr. Steel Res.* **2022**, *199*, 107573. [[CrossRef](#)]
107. Xie, L.; Wu, J.; Huang, Q. Experimental study on low-cycle fatigue performance of weld-free buckling-restrained braces. *J. Earthq. Eng.* **2018**, *22*, 1392–1414. [[CrossRef](#)]
108. Gu, T.; Li, J.H.; Sun, J.; Jia, L.J.; Liu, T.; Ge, H. Experimental study on miniature buckling-restrained brace with corrugated core bar. *J. Earthq. Eng.* **2022**, *26*, 6633–6655. [[CrossRef](#)]
109. Ebadi Jamkhaneh, M.; Homaioon Ebrahimi, A.; Shokri Amiri, M. Seismic performance of steel-braced frames with an all-steel buckling restrained brace. *Pract. Period. Struct. Des. Constr.* **2018**, *23*, 04018016. [[CrossRef](#)]
110. American Institute of Steel Construction. *Seismic Provisions for Structural Steel Buildings*; American Institute of Steel Construction: Chicago, IL, USA, 2002; Number 2.
111. Tsai, K.C.; Wu, A.C.; Wei, C.Y.; Lin, P.C.; Chuang, M.C.; Yu, Y.J. Welded end-slot connection and debonding layers for buckling-restrained braces. *Earthq. Eng. Struct. Dyn.* **2014**, *43*, 1785–1807. [[CrossRef](#)]
112. Chen, Q.; Wang, C.L.; Meng, S.; Zeng, B. Effect of the unbonding materials on the mechanic behavior of all-steel buckling-restrained braces. *Eng. Struct.* **2016**, *111*, 478–493. [[CrossRef](#)]
113. Chou, C.C.; Chen, S.Y. Subassembly tests and finite element analyses of sandwiched buckling-restrained braces. *Eng. Struct.* **2010**, *32*, 2108–2121. [[CrossRef](#)]
114. Wu, A.C.; Lin, P.C.; Tsai, K.C. High-mode buckling responses of buckling-restrained brace core plates. *Earthq. Eng. Struct. Dyn.* **2014**, *43*, 375–393. [[CrossRef](#)]
115. Palazzo, G.; López-Almansa, F.; Cahis, X.; Crisafulli, F. A low-tech dissipative buckling restrained brace. Design, analysis, production and testing. *Eng. Struct.* **2009**, *31*, 2152–2161. [[CrossRef](#)]
116. Genna, F.; Gelfi, P. Analysis of the lateral thrust in bolted steel buckling-restrained braces. I: Experimental and numerical results. *J. Struct. Eng.* **2012**, *138*, 1231–1243. [[CrossRef](#)]
117. Genna, F.; Gelfi, P. Analysis of the lateral thrust in bolted steel buckling-restrained braces. II: Engineering analytical estimates. *J. Struct. Eng.* **2012**, *138*, 1244–1254. [[CrossRef](#)]
118. Zhang, G.; Chen, P.; Zhao, Z.; Wu, J. Experimental study on seismic performance of rocking buckling-restrained brace steel frame with liftable column base. *J. Constr. Steel Res.* **2018**, *143*, 291–306. [[CrossRef](#)]
119. Gheidi, A.; Mirtaheri, M.; Zandi, A.P.; Alanjari, P. Effect of filler material on local and global behaviour of buckling-restrained braces. *Struct. Des. Tall Spec. Build.* **2011**, *20*, 700–710. [[CrossRef](#)]
120. Takeuchi, T.; Hajjar, J.; Matsui, R.; Nishimoto, K.; Aiken, I. Effect of local buckling core plate restraint in buckling restrained braces. *Eng. Struct.* **2012**, *44*, 304–311. [[CrossRef](#)]
121. Esfandiari, J.; Soleimani, E. Laboratory investigation on the buckling restrained braces with an optimal percentage of microstructure, polypropylene and hybrid fibers under cyclic loads. *Compos. Struct.* **2018**, *203*, 585–598. [[CrossRef](#)]
122. Alemayehu, R.W.; Kim, Y.; Park, M.J.; Park, M.; K. Ju, Y. Experimental and finite element study of polymer infilled tube-in-tube buckling restrained brace. *Metals* **2021**, *11*, 1358. [[CrossRef](#)]
123. Pathan, N.B.; Couch, L.; Tehrani, F.M.; Naghshineh, A.; Fischer, O. Experimental Seismic Evaluation of Novel Buckling-Restrained Braced Frames Containing Tire-Derived Aggregate Concrete. *CivilEng* **2023**, *4*, 551–566. [[CrossRef](#)]
124. Ghowsi, A.F.; Sahoo, D.R. Cyclic behavior of all-steel BRBs with bolted angle restrainers: Testing and numerical analysis. *J. Earthq. Eng.* **2023**, *27*, 362–388. [[CrossRef](#)]
125. Guo, Y.L.; Zhang, B.H.; Zhu, B.L.; Zhou, P.; Zhang, Y.H.; Tong, J.Z. Theoretical and experimental studies of battened buckling-restrained braces. *Eng. Struct.* **2017**, *136*, 312–328. [[CrossRef](#)]
126. Guo, Y.L.; Zhang, B.H.; Jiang, Z.Q.; Chen, H. Critical load and application of core-separated buckling-restrained braces. *J. Constr. Steel Res.* **2015**, *106*, 1–10. [[CrossRef](#)]
127. Zhu, B.L.; Guo, Y.L.; Zhou, P.; Bradford, M.A.; Pi, Y.L. Numerical and experimental studies of corrugated-web-connected buckling-restrained braces. *Eng. Struct.* **2017**, *134*, 107–124. [[CrossRef](#)]

128. Guo, Y.L.; Tong, J.Z.; Zhang, B.H.; Zhu, B.L.; Pi, Y.L. Theoretical and experimental investigation of core-separated buckling-restrained braces. *J. Constr. Steel Res.* **2017**, *135*, 137–149. [[CrossRef](#)]
129. Guo, Y.L.; Zhou, P.; Wang, M.Z.; Pi, Y.L.; Bradford, M.A.; Tong, J.Z. Experimental and numerical studies of hysteretic response of triple-truss-confined buckling-restrained braces. *Eng. Struct.* **2017**, *148*, 157–174. [[CrossRef](#)]
130. Guo, Y.L.; Zhou, P.; Wang, M.Z.; Pi, Y.L.; Bradford, M.A. Numerical studies of cyclic behavior and design suggestions on triple-truss-confined buckling-restrained braces. *Eng. Struct.* **2017**, *146*, 1–17. [[CrossRef](#)]
131. *GB50010-2010*; Code for Seismic Design of Buildings. China Architecture & Building Press: Beijing, China, 2010.
132. Zhu, B.L.; Guo, Y.L.; Zhou, P.; Pi, Y.L. Load-carrying performance and design of BRBs confined with longitudinal shuttle-shaped-trusses. *J. Constr. Steel Res.* **2020**, *167*, 105954. [[CrossRef](#)]
133. Guo, Y.L.; Zhu, J.S.; Zhou, P.; Zhu, B.L. A new shuttle-shaped buckling-restrained brace. Theoretical study on buckling behavior and load resistance. *Eng. Struct.* **2017**, *147*, 223–241. [[CrossRef](#)]
134. Luo, L.; Sun, X.; Song, X.; Ou, Z.; Zhang, L. Experimental and numerical study on the hysteretic behavior of a hybrid timber buckling-restrained brace with a cross-shaped steel core. *Soil Dyn. Earthq. Eng.* **2022**, *162*, 107461. [[CrossRef](#)]
135. Takeuchi, T.; Terazawa, Y.; Komuro, S.; Kurata, T.; Sittler, B. Performance and failure modes of mass timber buckling-restrained braces under cyclic loading. *Eng. Struct.* **2022**, *266*, 114462. [[CrossRef](#)]
136. Miller, D.J.; Fahnstock, L.A.; Eatherton, M.R. Development and experimental validation of a nickel–titanium shape memory alloy self-centering buckling-restrained brace. *Eng. Struct.* **2012**, *40*, 288–298. [[CrossRef](#)]
137. Wang, H.; Nie, X.; Pan, P. Development of a self-centering buckling restrained brace using cross-anchored pre-stressed steel strands. *J. Constr. Steel Res.* **2017**, *138*, 621–632. [[CrossRef](#)]
138. Zhang, H.; Quan, L.; Lu, X. Experimental hysteretic behavior and application of an assembled self-centering buckling-restrained brace. *J. Struct. Eng.* **2022**, *148*, 04021302. [[CrossRef](#)]
139. Zhou, Z.; Xie, Q.; Lei, X.; He, X.; Meng, S. Experimental investigation of the hysteretic performance of dual-tube self-centering buckling-restrained braces with composite tendons. *J. Compos. Constr.* **2015**, *19*, 04015011. [[CrossRef](#)]
140. Chen, L.; Wang, D.; Shi, F.; Zhang, R.; Sun, Z. Hysteretic performance of self-centering buckling-restrained braces with embedded friction spring. *Eng. Struct.* **2023**, *280*, 115595. [[CrossRef](#)]
141. Xiang, P.; Shi, M.; Jia, L.J.; Wu, M.; Wang, C.L. Constitutive model of aluminum under variable-amplitude cyclic loading and its application to buckling-restrained braces. *J. Mater. Civ. Eng.* **2018**, *30*, 04017304. [[CrossRef](#)]
142. Deng, K.; Pan, P.; Nie, X.; Xu, X.; Feng, P.; Ye, L. Study of GFRP steel buckling restraint braces. *J. Compos. Constr.* **2015**, *19*, 04015009. [[CrossRef](#)]
143. Dusicka, P.; Tinker, J. Global restraint in ultra-lightweight buckling-restrained braces. *J. Compos. Constr.* **2013**, *17*, 139–150. [[CrossRef](#)]
144. Sun, H.; Jia, M.; Zhang, S.; Wang, Y. Study of buckling-restrained braces with concrete infilled GFRP tubes. *Thin-Walled Struct.* **2019**, *136*, 16–33. [[CrossRef](#)]
145. Jia, M.; Yu, X.; Lu, D.; Lu, B. Experimental research of assembled buckling-restrained braces wrapped with carbon or basalt fiber. *J. Constr. Steel Res.* **2017**, *131*, 144–161. [[CrossRef](#)]
146. Zhao, J.; Wang, H.; Dong, J.; Zhang, L. Experimental Study of Maintenance-Free Steel-Composite Buckling Restrained Braces. *Materials* **2022**, *15*, 5538. [[CrossRef](#)] [[PubMed](#)]
147. *ANSI/AISC 341-10*; Seismic Provisions for Structural Steel Buildings. American Institute of Steel Construction: Chicago, IL, USA, 2010.

**Disclaimer/Publisher’s Note:** The statements, opinions and data contained in all publications are solely those of the individual author(s) and contributor(s) and not of MDPI and/or the editor(s). MDPI and/or the editor(s) disclaim responsibility for any injury to people or property resulting from any ideas, methods, instructions or products referred to in the content.